

Equation of state and
coarse grained free energy
for matrix models

J. BERGES*

and

C. WETTERICH†

*Institut für Theoretische Physik
Universität Heidelberg
Philosophenweg 16
69120 Heidelberg, Germany*

Abstract

We investigate phase transitions in three dimensional scalar matrix models, with special emphasis on complex 2×2 matrices. The universal equation of state for weak first order phase transitions is computed. We also study the coarse grained free energy. Its dependence on the coarse graining scale gives a quantitative criterion for the validity of the standard treatment of bubble nucleation.

*Email: J.Berges@thphys.uni-heidelberg.de

†Email: C.Wetterich@thphys.uni-heidelberg.de

1 Introduction

Matrix models are extensively discussed in statistical physics. Beyond the $O(N)$ symmetric Heisenberg models ('vector models') they correspond to the simplest scalar field theories. There is a wide set of different applications as the metal insulator transition [1] or liquid crystals [2] or strings and random surfaces [3] . . . The universal behavior of these models in the vicinity of a second order or weak first order phase transition is determined by the symmetries and the field content of the corresponding field theories. We will consider here models with $U(N) \times U(N)$ symmetry with a scalar field in the (\bar{N}, N) representation, described by an arbitrary complex $N \times N$ matrix φ . We do not impose nonlinear constraints for φ a priori but rather use a 'classical' potential. This enforces nonlinear constraints in certain limiting cases. Among those, our model describes a nonlinear matrix model for unitary matrices or one for singular 2×2 matrices. The universal critical behavior does not depend on the details of the classical potential and there is no difference between the linear and nonlinear models in the vicinity of the limiting cases. We concentrate in this paper on three dimensions, relevant for statistical physics and critical phenomena in high temperature field theory.

The cases $N = 2, 3$ have a relation to high temperature strong interaction physics. At vanishing temperature the four dimensional models can be used for a description of the pseudoscalar and scalar mesons for N quark flavors. For $N = 3$ the antihermitean part of φ describes here the pions, kaons, η and η' whereas the hermitean part accounts for the nonet of scalar 0^{++} mesons.¹ For nonzero temperature T the effects of fluctuations with momenta $p^2 \lesssim (2\pi T)^2$ are described by the corresponding three dimensional models. These models account for the long distance physics and obtain after integrating out the short distance fluctuations by virtue of dimensional reduction [5, 6, 7]. In particular, the three dimensional models embody the essential dynamics in the immediate vicinity of a second order or weak first order chiral phase transition [8]. The four dimensional models at nonvanishing temperature have also been used for investigations of the temperature dependence of meson masses [9, 10]. The simple model investigated in this paper is not yet realistic – it neglects the effect of the axial anomaly which reduces the chiral flavor symmetry to $SU(N) \times SU(N)$. It also accounts only for meson fluctuations and ignores, for example, the temperature dependence of the binding mechanism which gives rise to mesons as quark-antiquark bound states. Nevertheless, it should serve as an interesting starting point for a later analysis of more realistic effective three dimensional meson models arising in high temperature QCD. For simplicity we will concentrate here on $N = 2$, but our methods can be generalized to $N = 3$ and the inclusion of the axial anomaly.

The case $N = 2$ also has a relation to the electroweak phase transition in models with two Higgs doublets. Our model corresponds here to the critical behavior in a special class of left-right symmetric theories in the limit where the gauge couplings are neglected. Even though vanishing gauge couplings are not a good approximation for typical realistic models one would like to understand this limiting case reliably.

We are mainly interested in the character and the detailed physics of the phase transi-

¹See [4] for a recent phenomenological analysis.

tion. Standard (linear) high temperature perturbation theory can give a reliable description only if the relevant dimensionless couplings remain small near the phase transition. This requires two conditions: First, the effective three dimensional couplings evaluated for typical momenta $p^2 \simeq (2\pi T)^2$ must be small in units of temperature. For the example of a quartic coupling this means $\bar{\lambda}(2\pi T)/T \ll 1$. In high temperature field theory this ratio corresponds to the four dimensional coupling, e.g. $\bar{\lambda}(2\pi T) = \lambda_4 T$. The above condition is fulfilled whenever the four dimensional (or zero temperature) couplings remain perturbative. On the other hand, it never holds for nonlinear matrix models where the corresponding ratios diverge. The second condition requires the phase transition to be sufficiently strong first order. If we denote by m_c the relevant mass at the critical temperature, standard perturbation theory turns out to be actually an expansion in $\bar{\lambda}/m_c$ rather than $\bar{\lambda}/T$. For a given value of $\bar{\lambda}$ a perturbative expansion can therefore only converge if m_c is sufficiently large, $m_c \gg \lambda_4 T$. In consequence, perturbation theory is not applicable for the interesting cases of second order ($m_c = 0$) or weak first order ($m_c \ll \lambda_4 T$) phase transitions.

This property can also be understood in terms of running couplings. One may consider the model in presence of an infrared cutoff with typical scale k . Here k may be given by external conditions (as a finite volume) or induced by the problem studied (e.g. typical external momenta in vertices or a characteristic scale of critical bubbles in problems of bubble formation). One may also associate k with a relevant mass away from the critical temperature or for nonvanishing sources or external fields. Or else the infrared cutoff can be introduced as a purely technical tool. One can define running renormalized couplings $\bar{\lambda}_R(k)$ by appropriate renormalized n-point functions in presence of the infrared cutoff and study the flow of $\bar{\lambda}_R(k)$ as k is lowered. Often an originally small dimensionless ratio $\lambda(k) = \bar{\lambda}_R(k)/k$ increases in the course of the evolution. Perturbation theory breaks down when $\lambda(k)$ reaches values of order one. One needs nonperturbative methods to follow the flow for larger values of $\lambda(k)$ if k becomes small. This is typically what happens for a second order phase transition where one needs at the critical temperature the behavior for $k \rightarrow 0$. In this case the dimensionless coupling $\lambda(k)$ reaches a fixed point λ_* which is for most simple models substantially larger than one. For the present matrix models one wants to know if the phase transition becomes second order in certain regions of parameter space. This is equivalent to the question if the system of running couplings admits a fixed point which is infrared stable (except one relevant direction corresponding to $T - T_c$). Clearly, this is a nonperturbative question. It can be addressed by an expansion in $\epsilon = 4 - d$ [11, 12]. However, the reliability of this expansion is not guaranteed a priori since for three dimensions $\epsilon = 1$ is not a small parameter. We will employ here a method which is based on the general concepts of the Wilsonian renormalization group [13, 14]. More precisely, we study an approximate solution to an exact flow equation for a coarse grained free energy. We find that the phase transition for the investigated matrix models with $N = 2$ and symmetry breaking pattern $U(2) \times U(2) \rightarrow U(2)$ is always (fluctuation induced) first order, except for a boundary case with enhanced $O(8)$ symmetry. For a large part of parameter space the transition is weak and one finds large renormalized dimensionless couplings near the critical temperature. If the running of the couplings

towards approximate fixed points (there are no exact fixed points) is sufficiently fast the large distance physics loses memory of the details of the short distance or classical action. In this case the physics near the phase transition is described by an universal equation of state.

Besides the possible practical applications it is a theoretical challenge to find the universal equation of state for weak first order phase transitions. For the second order phase transition in $O(N)$ symmetric vector models (Heisenberg models) this has only recently been achieved [15] by the method employed here and confirmed by numerical lattice simulations [16]. Whereas for second order transitions the universal equation of state can be expressed as a function of only one scaling variable, the additional scale m_c in a first order transition induces a second dimensionless ratio. The equation of state or, equivalently, the effective potential or free energy therefore depends on two different scaling variables in the universal region. We have succeeded to solve this problem for the present matrix models and present the universal equation of state in sect. 8.

Another old and challenging problem for first order phase transitions concerns the question of the validity of Langer's theory of bubble formation [17]. This requires first a meaningful definition of a coarse grained free energy with a coarse graining scale k and second the validity of a saddle point approximation for the treatment of fluctuations around the critical bubble. Here only fluctuations with momenta smaller than k must be included. We will see that the two issues are closely related. The validity of the saddle point approximation typically requires small dimensionless couplings $\lambda(k)$. On the other hand we observe for large $\lambda(k)$ that the form of the coarse grained effective potential U_k depends strongly on k even for scales k where the location of the minima of U_k is essentially independent of k . This means that the lowest order in the saddle point approximation (classical contribution) depends strongly on the details of the coarse graining procedure. Since the final results as tunneling rates etc. must be independent of the coarse graining prescription this is only compatible with a large contribution from the higher orders of the saddle point expansion. Section 9 deals with this issue in a quantitative way.

Our paper is organized as follows. The nonperturbative method we employ relies on an exact flow equation for the effective average action Γ_k which is introduced in section 2. In section 3 we define the $U(2) \times U(2)$ symmetric matrix model and we establish the connection to a matrix model for unitary matrices and to one for singular complex 2×2 matrices. There we also give an interpretation of the model as the coupled system of two $SU(2)$ -doublets for the weak interaction Higgs sector. Section 4 is devoted to an overview over the phase structure and the coarse grained effective potential U_k for the three dimensional theory. The evolution equation for U_k and its scaling form is computed in section 5. A method for its numerical solution is discussed in section 6 which also contains the flow equation for the wave function renormalization constant or the anomalous dimension η . A detailed account on the renormalization group flow is presented in section 7. We compute the universal form of the equation of state for weak first order phase transitions in section 8 and we extract critical exponents and the corresponding index relations. The dependence of the coarse grained effective potential on the coarse graining scale is studied in detail in section 9. The quantitative analysis is

applied to Langer's theory of bubble formation. Section 10 contains the conclusions and an outlook.

2 Effective average action

The effective average action Γ_k [18, 19] is a coarse grained free energy with an infrared cutoff or a coarse graining scale $\sim k$. More precisely, for a theory described by a classical action S , the effective average action results from the integration of degrees of freedom with characteristic momenta larger than k . To be explicit we consider a k -dependent generating functional with N^2 complex scalar fields χ_{ab} ($a, b = 1 \dots N$)

$$W_k[j] = \ln \int D\chi \exp \left(-S[\chi] - \Delta_k S[\chi] + \frac{1}{2} \int d^d x \left(j_{ab}^*(x) \chi^{ab}(x) + \chi_{ab}^*(x) j^{ab}(x) \right) \right) \quad (2.1)$$

with S the classical action and j_{ab} arbitrary sources. The scale dependence arises from the introduction of an additional infrared cutoff term

$$\Delta_k S[\chi] = \int \frac{d^d q}{(2\pi)^d} R_k(q) \chi_{ab}^*(q) \chi^{ab}(q). \quad (2.2)$$

Without this term W_k becomes the usual generating functional for the connected Green functions. Here the infrared cutoff function R_k is required to vanish for $k \rightarrow 0$ and to diverge for $k \rightarrow \infty$ and fixed q^2 . This can be achieved, for example, by the choice

$$R_k(q) = \frac{Z_k q^2 e^{-q^2/k^2}}{1 - e^{-q^2/k^2}} \quad (2.3)$$

where Z_k denotes an appropriate wave function renormalization constant which will be defined below. For fluctuations with small momenta $q^2 \ll k^2$ the cutoff $R_k \simeq Z_k k^2$ acts like an additional mass term and prevents their propagation. For $q^2 \gg k^2$ the infrared cutoff vanishes such that the functional integration of the high momentum modes is not disturbed. The expectation value of χ in the presence of $\Delta_k S[\chi]$ and j reads $\varphi^{ab} \equiv \langle \chi^{ab} \rangle = 2 \delta W_k[j] / \delta j_{ab}^*$. We define the effective average action via a Legendre transform

$$\Gamma_k[\varphi] = -W_k[j] + \frac{1}{2} \int d^d x \left(j_{ab}^*(x) \chi^{ab}(x) + \chi_{ab}^*(x) j^{ab}(x) \right) - \Delta_k S[\varphi]. \quad (2.4)$$

As a consequence, as the scale k is lowered Γ_k interpolates from the classical action $S = \lim_{k \rightarrow \infty} \Gamma_k$ to the standard effective action $\Gamma = \lim_{k \rightarrow 0} \Gamma_k$, i.e. the generating functional of $1PI$ Green functions [19]. Lowering k results in a successive inclusion of fluctuations with momenta $q^2 \gtrsim k^2$ and therefore permits to explore the theory on larger and larger length scales. One can view Γ_k as the effective action for averages of fields over a volume of size $\sim k^{-d}$ and the approach is similar in spirit to the block spin action [13, 14] on the lattice. The interpolation property of Γ_k can be used to 'start' at some high momentum scale Λ where Γ_Λ can be taken as the classical or short distance action and to solve the

theory by following Γ_k to $k \rightarrow 0$. The scale dependence of Γ_k can be described by an exact nonperturbative evolution equation [19, 20, 21, 22]

$$\frac{\partial}{\partial t} \Gamma_k[\varphi] = \frac{1}{2} \text{Tr} \left\{ \left(\Gamma_k^{(2)}[\varphi] + R_k \right)^{-1} \frac{\partial R_k}{\partial t} \right\} \quad (2.5)$$

where $t = \ln(k/\Lambda)$. The evolution is described in terms of the *exact* inverse propagator $\Gamma_k^{(2)}$ as given by the second functional derivative of Γ_k with respect to the fields. The trace involves a momentum integration as well as a summation over the internal indices which count the $2N^2$ real scalar fields contained in φ . The additional cutoff function R_k with a form like the one given above renders the momentum integration both infrared (IR) and ultraviolet (UV) finite. In particular, the direct implementation of the additional mass term $R_k \simeq Z_k k^2$ for $q^2 \ll k^2$ into the inverse average propagator makes the formulation suitable for dealing with theories which are plagued by infrared problems in perturbation theory. The flow equation (2.5) is compatible with all symmetries of the model and can be generalized to include possible local gauge symmetries [23]. The exact renormalization group equation can be formulated in many different but formally equivalent ways [14, 24] and it may be interpreted as a differential form of the Schwinger-Dyson equations [25].

From its construction, i.e. the inclusion of fluctuations with characteristic momenta larger than a given infrared cutoff $\sim k$, the effective average action is the appropriate quantity for the study of physics at a scale k . It therefore realizes the concept of a coarse grained free energy in the sense of ref. [17]. Such a quantity becomes especially desirable for a description of first order phase transitions. In contrast to a second order phase transition there is an inherent length scale l_0 due to a finite correlation length at a first order phase transition. This length scale acts as a physical infrared cutoff. The coarse grained effective action Γ_k with $k \sim l_0^{-1}$ accounts for all fluctuations with momenta larger than this physical infrared cutoff and it is the appropriate quantity for the study of the physics at the scale l_0 . To be explicit, one may consider the coarse grained effective potential U_k . It is obtained from the coarse grained effective action Γ_k for a constant field φ . At a first order phase transition there is a nonzero difference between the field expectation value (order parameter) in the symmetric (disordered) and in the spontaneously broken (ordered) phase. The two phases correspond to two different minima of the coarse grained effective potential U_k and both minima are separated by a potential barrier. The coarse grained potential U_k is therefore a nonconvex function whereas the standard effective potential $U = \lim_{k \rightarrow 0} U_k$ has to be convex by its definition as a Legendre transform. The convexity is due to the effect of fluctuations with characteristic length scales larger than l_0 [26]. The study of physical processes such as tunneling or inflation usually relies on the nonconvex part of the potential which is discussed in section 9.

Though the evolution equation (2.5) for the effective average action is exact, it remains a complicated functional differential equation. In practice one has to find a truncation for Γ_k in order to obtain approximate solutions. An important feature of the exact flow equation is therefore its simple and intuitive form which helps to find a nonperturbative approximation scheme. The r.h.s. of eq. (2.5) expresses the scale dependence of Γ_k in terms of the exact propagator. Known properties of the propagator can be used as a

guide to find an appropriate truncation for the effective average action. For a scalar theory the propagator is a matrix characterized by mass terms and kinetic terms $\sim Zq^2$. The mass matrix is given by the second derivative of the potential U_k with respect to the fields. In general Z can be a complicated function of the fields and momenta. We may exploit the fact that the function Z plays the role of a field and momentum dependent wave function renormalization. For second order phase transitions and approximately for weak first order phase transitions the behavior of Z is governed by the anomalous dimension η . Typically for three and four dimensional scalar theories η is small. (In our case the relevant value is $\eta \simeq 0.022$ as given by the corresponding index in the $O(8)$ symmetric Heisenberg model). One therefore expects a weak dependence of Z on the fields and momenta. We will exploit this in the following.

3 $U(2) \times U(2)$ symmetric scalar matrix model

We consider a $U(2) \times U(2)$ symmetric effective action for a scalar field φ which transforms in the $(2, 2)$ representation with respect to the subgroup $SU(2) \times SU(2)$. Here φ is represented by a complex 2×2 matrix and the transformations are

$$\begin{aligned}\varphi &\rightarrow U\varphi V^\dagger, \\ \varphi^\dagger &\rightarrow V\varphi^\dagger U^\dagger\end{aligned}\tag{3.1}$$

where U and V are unitary 2×2 matrices corresponding to the two distinct $U(2)$ factors.

We classify the invariants for the construction of the effective average action by the number of derivatives. The lowest order in a systematic derivative expansion [27, 22] of Γ_k is given by

$$\Gamma_k = \int d^d x \left\{ U_k(\varphi, \varphi^\dagger) + Z_k \partial_\mu \varphi_{ab}^* \partial^\mu \varphi^{ab} \right\} \quad (a, b = 1, 2).\tag{3.2}$$

The term with no derivatives defines the scalar potential U_k which is an arbitrary function of traces of powers of $\varphi^\dagger \varphi$. The most general $U(2) \times U(2)$ symmetric scalar potential can be expressed as a function of only two independent invariants,

$$\begin{aligned}\rho &= \text{tr}(\varphi^\dagger \varphi) \\ \tau &= 2 \text{tr} \left(\varphi^\dagger \varphi - \frac{1}{2} \rho \right)^2 = 2 \text{tr}(\varphi^\dagger \varphi)^2 - \rho^2.\end{aligned}\tag{3.3}$$

Here we have used for later convenience the traceless matrix $\varphi^\dagger \varphi - \frac{1}{2} \rho$ to construct the second invariant. Higher invariants, $\text{tr} \left(\varphi^\dagger \varphi - \frac{1}{2} \rho \right)^n$ for $n > 2$, can be expressed as functions of ρ and τ [28].

For the derivative part we consider a standard kinetic term with a scale dependent wave function renormalization constant Z_k . The first correction to the kinetic term would include field dependent wave function renormalizations $Z_k(\rho, \tau)$ plus functions not specified in eq. (3.2) which account for a different index structure of invariants with two

derivatives. These wave function renormalizations may be defined at zero momentum. The next level involves invariants with four derivatives and so on. We define Z_k at the minimum ρ_0, τ_0 of U_k and at vanishing momenta q^2 ,

$$Z_k = Z_k(\rho = \rho_0, \tau = \tau_0; q^2 = 0). \quad (3.4)$$

The factor Z_k appearing in the definition of the infrared cutoff R_k in eq. (2.3) is identified with (3.4). The k -dependence of this function is given by the anomalous dimension

$$\eta(k) = -\frac{d}{dt} \ln Z_k. \quad (3.5)$$

If the ansatz (3.2) is inserted into the flow equation for the effective average action (2.5) one obtains flow equations for the effective average potential $U_k(\rho, \tau)$ and for the wave function renormalization constant Z_k (or equivalently the anomalous dimension η). This is done in sections 5 and 6. These flow equations have to be integrated starting from some short distance scale Λ and one has to specify U_Λ and Z_Λ as initial conditions. At the scale Λ , where Γ_Λ can be taken as the classical or short distance action, no integration of fluctuations has been performed. The short distance potential is taken to be a quartic potential which is parametrized by two quartic couplings $\bar{\lambda}_{1\Lambda}, \bar{\lambda}_{2\Lambda}$ and a mass term. We start in the spontaneously broken regime where the minimum of the potential occurs at a nonvanishing field value and there is a negative mass term at the origin of the potential ($\bar{\mu}_\Lambda^2 > 0$),

$$U_\Lambda(\rho, \tau) = -\bar{\mu}_\Lambda^2 \rho + \frac{1}{2} \bar{\lambda}_{1\Lambda} \rho^2 + \frac{1}{4} \bar{\lambda}_{2\Lambda} \tau \quad (3.6)$$

and $Z_\Lambda = 1$. The potential is bounded from below provided $\bar{\lambda}_{1\Lambda} > 0$ and $\bar{\lambda}_{2\Lambda} > -2\bar{\lambda}_{1\Lambda}$. For $\bar{\lambda}_{2\Lambda} > 0$ one observes the potential minimum for the configuration $\varphi_{ab} = \varphi \delta_{ab}$ corresponding to the spontaneous symmetry breaking down to the diagonal $U(2)$ subgroup of $U(2) \times U(2)$. For negative $\bar{\lambda}_{2\Lambda}$ the potential is minimized by the configuration $\varphi_{ab} = \varphi \delta_{a1} \delta_{ab}$ which corresponds to the symmetry breaking pattern $U(2) \times U(2) \rightarrow U(1) \times U(1) \times U(1)$. In the special case $\bar{\lambda}_{2\Lambda} = 0$ the theory exhibits an enhanced $O(8)$ symmetry. This constitutes the boundary between two phases with different symmetry breaking patterns.

The limits of infinite couplings correspond to nonlinear constraints in the matrix model. For $\bar{\lambda}_{1\Lambda} \rightarrow \infty$ with fixed ratio $\bar{\mu}_\Lambda^2 / \bar{\lambda}_{1\Lambda}$ one finds the constraint $\text{tr}(\varphi^\dagger \varphi) = 2\bar{\mu}_\Lambda^2 / \bar{\lambda}_{1\Lambda}$. By a convenient choice of Z_Λ (rescaling of φ) this can be brought to the form $\text{tr}(\varphi^\dagger \varphi) = 2$. On the other hand, the limit $\bar{\lambda}_{2\Lambda} \rightarrow +\infty$ enforces the constraint $\varphi^\dagger \varphi = \frac{1}{2} \text{tr}(\varphi^\dagger \varphi)$. Combining the limits $\bar{\lambda}_{1\Lambda} \rightarrow \infty, \bar{\lambda}_{2\Lambda} \rightarrow \infty$ the constraint reads $\varphi^\dagger \varphi = 1$ and we deal with a matrix model for unitary matrices. (These considerations generalize to arbitrary N .) Another interesting limit obtains for $\bar{\lambda}_{1\Lambda} = -\frac{1}{2} \bar{\lambda}_{2\Lambda} + \Delta_\lambda, \Delta_\lambda > 0$ if $\bar{\lambda}_{2\Lambda} \rightarrow -\infty$. In this case the nonlinear constraint reads $(\text{tr} \varphi^\dagger \varphi)^2 = \text{tr}(\varphi^\dagger \varphi)^2$ which implies for $N = 2$ that $\det \varphi = 0$. This is a matrix model for singular complex 2×2 matrices.

One can also interpret our model as the coupled system of two $SU(2)$ -doublets for the weak interaction Higgs sector. This is simply done by decomposing the matrix φ_{ab} into

two two-component complex fundamental representations of one of the $SU(2)$ subgroups, $\varphi_{ab} \rightarrow \varphi_{1b}, \varphi_{2b}$. The present model corresponds to a particular left-right symmetric model with interactions specified by

$$\begin{aligned}\rho &= \varphi_1^\dagger \varphi_1 + \varphi_2^\dagger \varphi_2 \\ \tau &= \left(\varphi_1^\dagger \varphi_1 - \varphi_2^\dagger \varphi_2\right)^2 + 4\left(\varphi_1^\dagger \varphi_2\right)\left(\varphi_2^\dagger \varphi_1\right).\end{aligned}\tag{3.7}$$

We observe that for a typical weak interaction symmetry breaking pattern the expectation values of φ_1 and φ_2 should be aligned in the same direction or one of them should vanish. In the present model this corresponds to the choice $\bar{\lambda}_{2\Lambda} < 0$. The phase structure of a related model without the term $\sim (\varphi_1^\dagger \varphi_2)(\varphi_2^\dagger \varphi_1)$ has been investigated previously [29] and shows second or first order transitions². Combining these results with the outcome of this work leads already to a detailed qualitative overview over the phase pattern in a more general setting with three independent couplings for the quartic invariants $(\varphi_1^\dagger \varphi_1 + \varphi_2^\dagger \varphi_2)^2$, $(\varphi_1^\dagger \varphi_1 - \varphi_2^\dagger \varphi_2)^2$ and $(\varphi_1^\dagger \varphi_2)(\varphi_2^\dagger \varphi_1)$. We also note that the special case $\bar{\lambda}_{2\Lambda} = 2\bar{\lambda}_{1\Lambda}$ corresponds to two Heisenberg models interacting only by a term sensitive to the alignment between φ_1 and φ_2 , i.e. a quartic interaction of the form $(\varphi_1^\dagger \varphi_1)^2 + (\varphi_2^\dagger \varphi_2)^2 + 2(\varphi_1^\dagger \varphi_2)(\varphi_2^\dagger \varphi_1)$.

The model is now completely specified and it remains to extract the flow equations for U_k and Z_k . Before this is carried out in sections 5 and 6 we present an overview over the phase structure in the next section. These results are obtained from a numerical solution of the evolution equations.

4 Phase structure

In this section we consider the $U(2) \times U(2)$ symmetric model in three space dimensions. The aim is to give an overview of our results concerning the phase structure and the effective average potential. We concentrate here on the spontaneous symmetry breaking with a residual $U(2)$ symmetry group. This symmetry breaking can be observed for a configuration which is proportional to the identity and with (3.3) one finds $\tau = 0$. In this case we shall use an expansion of $U_k(\rho, \tau)$ around $\tau = 0$ keeping only the linear term in τ . This amounts to assuming

$$\frac{\partial^n U_k}{\partial \tau^n}(\rho, \tau = 0) = 0 \quad \text{for } n \geq 2.\tag{4.1}$$

We will motivate this truncation in section 6 where we present a more detailed analysis. We make no expansion of $U_k(\rho, \tau)$ in terms of ρ . This allows the description of a first order phase transition where a second local minimum of $U_k(\rho) \equiv U_k(\rho, \tau = 0)$ appears. The ρ -dependence also gives information about the equation of state of the system.

For the considered symmetry breaking pattern the short distance potential U_Λ given in eq. (3.6) is parametrized by positive quartic couplings,

$$\bar{\lambda}_{1\Lambda}, \bar{\lambda}_{2\Lambda} > 0\tag{4.2}$$

²First order phase transitions and coarse graining have also been discussed in a multi-scalar model with Z_2 symmetry [30].

and the location of its minimum is given by

$$\rho_{0\Lambda} = \bar{\mu}_\Lambda^2 / \bar{\lambda}_{1\Lambda}. \quad (4.3)$$

To study the phase structure of the model we integrate the flow equation for the effective average potential U_k (cf. sect. 5, 6) for a variety of initial conditions $\rho_{0\Lambda}$, $\bar{\lambda}_{1\Lambda}$ and $\bar{\lambda}_{2\Lambda}$. In particular, for general $\bar{\lambda}_{1\Lambda}, \bar{\lambda}_{2\Lambda} > 0$ we are able to find a critical value $\rho_{0\Lambda} = \rho_{0c}$ for which the system exhibits a first order phase transition. In this case the evolution of U_k leads at some scale $k_2 < \Lambda$ to the appearance of a second local minimum at the origin of the effective average potential and both minima become degenerate in the limit $k \rightarrow 0$. If $\rho_0(k) > 0$ denotes the k -dependent outer minimum of the potential ($U'_k(\rho_0) = 0$, where the prime on U_k denotes the derivative with respect to ρ at fixed k) at a first order phase transition one has

$$\lim_{k \rightarrow 0} (U_k(0) - U_k(\rho_0)) = 0. \quad (4.4)$$

A measure of the distance from the phase transition is the difference $\delta\kappa_\Lambda = (\rho_{0\Lambda} - \rho_{0c})/\Lambda$. If $\bar{\mu}_\Lambda^2$ and therefore $\rho_{0\Lambda}$ is interpreted as a function of temperature, the deviation $\delta\kappa_\Lambda$ is proportional to the deviation from the critical temperature T_c , i.e. $\delta\kappa_\Lambda = A(T)(T_c - T)$ with $A(T_c) > 0$.

We consider in the following the effective average potential U_k for a nonzero scale k . This allows to observe the nonconvex part of the potential (cf. sect. 9). As an example we show in fig. 1 the effective average potential $U_{k=k_f}$ for $\lambda_{1\Lambda} = \bar{\lambda}_{1\Lambda}/\Lambda = 0.1$ and $\lambda_{2\Lambda} = \bar{\lambda}_{2\Lambda}/\Lambda = 2$ as a function of the renormalized field $\varphi_R = (\rho_R/2)^{1/2}$ with $\rho_R = Z_{k=k_f}\rho$. The scale k_f is some characteristic scale below which the location of the minimum $\rho_0(k)$ becomes essentially independent of k . Its precise definition is given below. We have normalized U_{k_f} and φ_R to powers of the renormalized minimum $\varphi_{0R}(k_f) = (\rho_{0R}(k_f)/2)^{1/2}$ with $\rho_{0R}(k_f) = Z_{k_f}\rho_0(k_f)$. The potential is shown for various values of deviations from the critical temperature or $\delta\kappa_\Lambda$. For the given examples $\delta\kappa_\Lambda = -0.03, -0.015$ the minimum at the origin becomes the absolute minimum and the system is in the symmetric (disordered) phase. Here φ_{0R} denotes the minimum in the metastable ordered phase. In contrast, for $\delta\kappa_\Lambda = 0.04, 0.1$ the absolute minimum is located at $\varphi_R/\varphi_{0R} = 1$ which characterizes the spontaneously broken phase. For large enough $\delta\kappa_\Lambda$ the local minimum at the origin vanishes. For $\delta\kappa_\Lambda = 0$ the two distinct minima are degenerate in height³. As a consequence the order parameter makes a discontinuous jump at the phase transition which characterizes the transition to be first order. It is instructive to consider some characteristic values of the effective average potential. In fig. 2 we consider for $\lambda_{1\Lambda} = 0.1, \lambda_{2\Lambda} = 2$ the value of the renormalized minimum $\rho_{0R}(k_f)$ and the radial mass term as a function of $-\delta\kappa_\Lambda$ or temperature. In the spontaneously broken phase the renormalized radial mass squared is given by (cf. section 5)

$$m_R^2(k_f) = 2Z_{k_f}^{-1}\rho_0 U''_{k_f}(\rho_0), \quad (4.5)$$

³We note that the critical temperature is determined by condition (4.4) in the limit $k \rightarrow 0$. Nevertheless for the employed nonvanishing scale $k = k_f$ the minima of U_k become almost degenerate at the critical temperature.

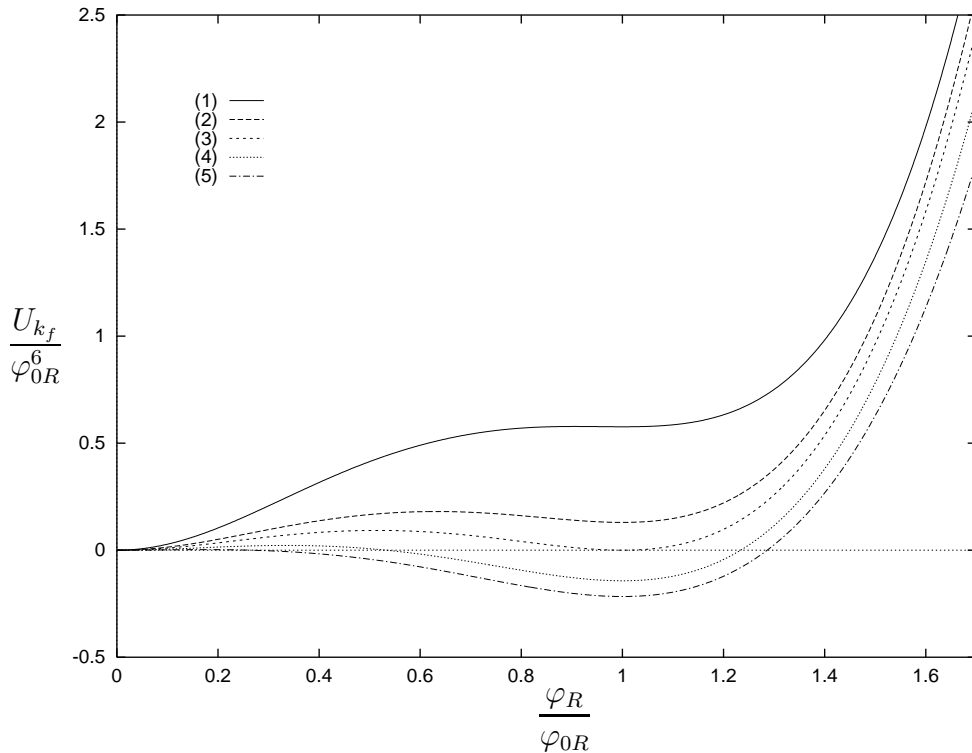


Figure 1: The effective average potential $U_{k=k_f}$ as a function of the renormalized field φ_R . The potential is shown for various values of $\delta\kappa_\Lambda \sim T_c - T$. The parameters for the short distance potential U_Λ are (1) $\delta\kappa_\Lambda = -0.03$, (2) $\delta\kappa_\Lambda = -0.015$, (3) $\delta\kappa_\Lambda = 0$, (4) $\delta\kappa_\Lambda = 0.04$, (5) $\delta\kappa_\Lambda = 0.1$ and $\lambda_{1\Lambda} = 0.1$, $\lambda_{2\Lambda} = 2$.

in the symmetric phase the renormalized mass term reads

$$m_{0R}^2(k_f) = Z_{k_f}^{-1} U'_{k_f}(0). \quad (4.6)$$

At the critical temperature ($\delta\kappa_\Lambda = 0$) one observes the discontinuity $\Delta\rho_{0R} = \rho_{0R}(k_f)$ and the jump in the mass term $\Delta m_R = m_R(k_f) - m_{0R}(k_f) = m_R^c - m_{0R}^c$. (Here the index 'c' denotes $\delta\kappa_\Lambda = 0$). The ratio $\Delta\rho_{0R}/\Lambda$ is a rough measure for the 'strength' of the first order transition. For $\Delta\rho_{0R}/\Lambda \ll 1$ the phase transition is weak in the sense that typical masses are small compared to Λ . In consequence, the long-wavelength fluctuations play a dominant role and the system exhibits universal behavior, i.e. it becomes largely independent of the details at the short distance scale Λ^{-1} . We will discuss the universal behavior in more detail below.

In order to characterize the strength of the phase transition for arbitrary positive values of $\lambda_{1\Lambda}$ and $\lambda_{2\Lambda}$ we consider lines of constant $\Delta\rho_{0R}/\Lambda$ in the $\lambda_{1\Lambda}, \lambda_{2\Lambda}$ plane. In fig. 3 this is done for the logarithms of these quantities. For fixed $\lambda_{2\Lambda}$ one observes that the discontinuity at the phase transition weakens with increased $\lambda_{1\Lambda}$. On the other hand for given $\lambda_{1\Lambda}$ one finds a larger jump in the order parameter for increased $\lambda_{2\Lambda}$. This is true up to a saturation point where $\Delta\rho_{0R}/\Lambda$ becomes independent of $\lambda_{2\Lambda}$. In the plot this can be observed from the vertical part of the line of constant $\ln(\Delta\rho_{0R}/\Lambda)$. This phenomenon

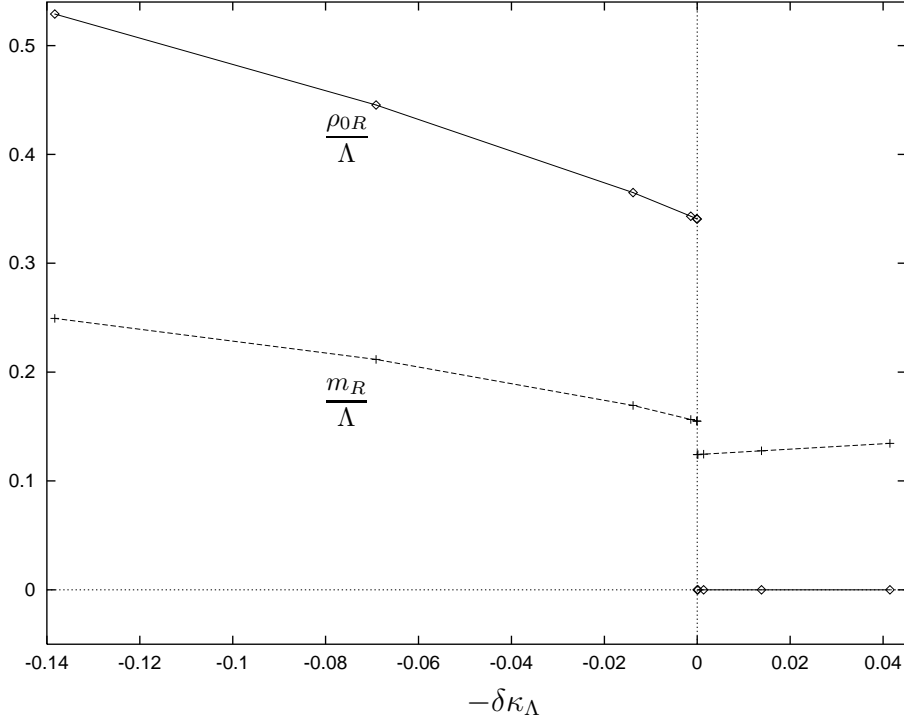


Figure 2: The minimum ρ_{0R} and the mass term m_R in units of the momentum scale Λ as a function of $-\delta\kappa_\Lambda$ or temperature ($\lambda_{1\Lambda} = 0.1$, $\lambda_{2\Lambda} = 2$, $k = k_f$). For $\delta\kappa_\Lambda = 0$ one observes the jump in the renormalized order parameter $\Delta\rho_{0R}$ and mass Δm_R .

occurs for arbitrary nonvanishing $\Delta\rho_{0R}/\Lambda$ in the strong $\lambda_{2\Lambda}$ coupling limit and is discussed in section 7.

In the following we give a detailed quantitative description of the first order phase transitions and a separation in weak and strong transitions. We consider some characteristic quantities for the effective average potential in dependence on the short distance parameters $\lambda_{1\Lambda}$ and $\lambda_{2\Lambda}$ for $\delta\kappa_\Lambda = 0$. We consider the discontinuity in the renormalized order parameter $\Delta\rho_{0R}$ and the inverse correlation lengths (mass terms) m_R^c and m_{0R}^c in the ordered and the disordered phase respectively. Fig. 4 shows the logarithm of $\Delta\rho_{0R}$ in units of Λ as a function of the logarithm of the initial coupling $\lambda_{2\Lambda}$. We have connected the calculated values obtained for various fixed $\lambda_{1\Lambda} = 0.1$, 2 and $\lambda_{1\Lambda} = 4$ by straight lines. The values are listed in table 1. For $\lambda_{2\Lambda}/\lambda_{1\Lambda} \lesssim 1$ the curves show constant positive slope. In this range $\Delta\rho_{0R}$ follows a power law behavior

$$\Delta\rho_{0R} = R(\lambda_{2\Lambda})^\theta, \quad \theta = 1.93. \quad (4.7)$$

The critical exponent θ is obtained from the slope of the curve in fig. 4 for $\lambda_{2\Lambda}/\lambda_{1\Lambda} \ll 1$. The exponent is universal and, therefore, does not depend on the specific value for $\lambda_{1\Lambda}$. On the other hand, the amplitude R grows with decreasing $\lambda_{1\Lambda}$. For vanishing $\lambda_{2\Lambda}$ the order parameter changes continuously at the transition point and one observes a second order phase transition as expected for the $O(8)$ symmetric vector model. As $\lambda_{2\Lambda}/\lambda_{1\Lambda}$

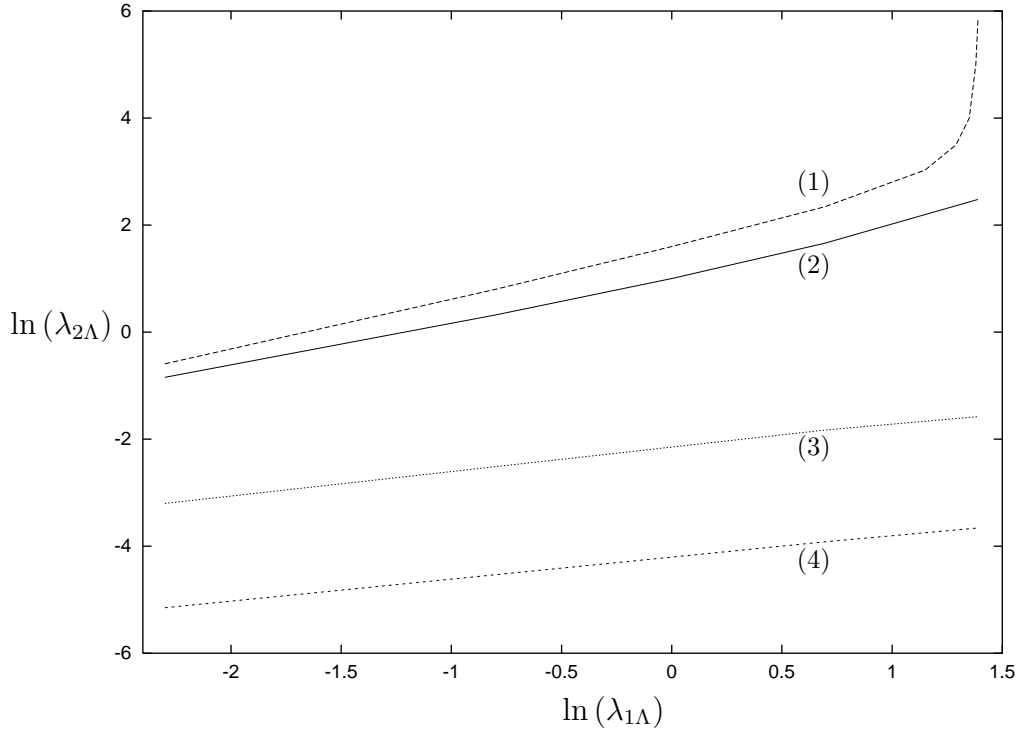


Figure 3: Lines of constant jump of the renormalized order parameter $\Delta\rho_{0R}/\Lambda$ at the phase transition in the $\ln(\lambda_{1\Lambda}), \ln(\lambda_{2\Lambda})$ plane. The curves correspond to (1) $\ln(\Delta\rho_{0R}/\Lambda) = -4.0$, (2) $\ln(\Delta\rho_{0R}/\Lambda) = -4.4$, (3) $\ln(\Delta\rho_{0R}/\Lambda) = -10.2$, (4) $\ln(\Delta\rho_{0R}/\Lambda) = -14.3$.

becomes larger than one the curves deviate substantially from the linear behavior. The deviation depends on the specific choice of the short distance potential. For $\lambda_{2\Lambda}/\lambda_{1\Lambda} \gg 1$ the curves flatten. In this range $\Delta\rho_{0R}$ becomes insensitive to a variation of the quartic coupling $\lambda_{2\Lambda}$.

In addition to the jump in the order parameter we present the mass terms m_R^c and m_{0R}^c which we normalize to $\Delta\rho_{0R}$. In fig. 5 these ratios are plotted versus the logarithm of the ratio of the initial quartic couplings $\lambda_{2\Lambda}/\lambda_{1\Lambda}$. Again values obtained for fixed $\lambda_{1\Lambda} = 0.1, 2$ and $\lambda_{1\Lambda} = 4$ are connected by straight lines. The universal range is set by the condition $m_R^c/\Delta\rho_{0R} \simeq \text{const}$ (equivalently for $m_{0R}^c/\Delta\rho_{0R}$). The universal ratios are $m_R^c/\Delta\rho_{0R} = 1.69$ and $m_{0R}^c/\Delta\rho_{0R} = 1.26$ as can be seen from table 1. For the given curves universality holds approximately for $\lambda_{2\Lambda}/\lambda_{1\Lambda} \lesssim 1/2$ and becomes 'exact' in the limit $\lambda_{2\Lambda}/\lambda_{1\Lambda} \rightarrow 0$. In this range we obtain

$$m_R^c = S(\lambda_{2\Lambda})^\theta, \quad m_{0R}^c = \tilde{S}(\lambda_{2\Lambda})^\theta. \quad (4.8)$$

The universal features of the system are not restricted to the weak coupling region of $\lambda_{2\Lambda}$. This is demonstrated in fig. 5 for values up to $\lambda_{2\Lambda} \simeq 2$. The ratios $m_R^c/\Delta\rho_{0R}$ and $m_{0R}^c/\Delta\rho_{0R}$ deviate from the universal values as $\lambda_{2\Lambda}/\lambda_{1\Lambda}$ is increased. For fixed $\lambda_{2\Lambda}$ a larger $\lambda_{1\Lambda}$ results in a weaker transition concerning $\Delta\rho_{0R}/\Lambda$. The ratio $m_R^c/\Delta\rho_{0R}$ increases with $\lambda_{1\Lambda}$ for small fixed $\lambda_{2\Lambda}$ whereas in the asymptotic region, $\lambda_{2\Lambda}/\lambda_{1\Lambda} \gg 1$, one observes from

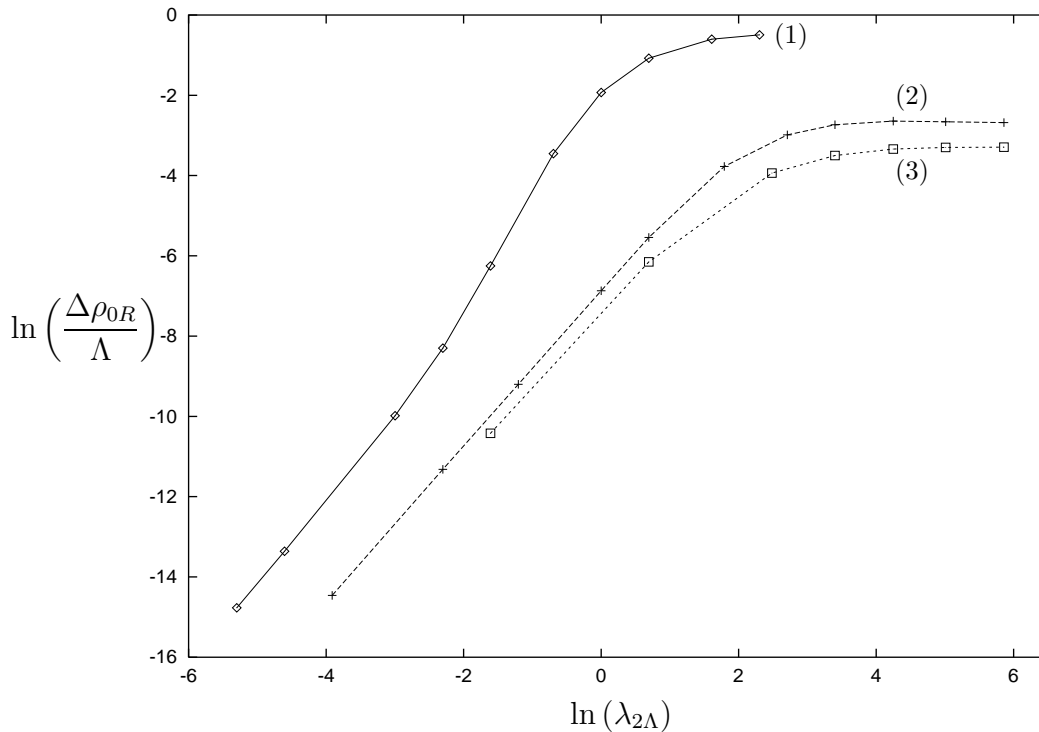


Figure 4: The logarithm of the discontinuity of the renormalized order parameter $\Delta\rho_{0R}/\Lambda$ as a function of $\ln(\lambda_{2\Lambda})$. Data points for fixed (1) $\lambda_{1\Lambda} = 0.1$, (2) $\lambda_{1\Lambda} = 2$, (3) $\lambda_{1\Lambda} = 4$ are connected by straight lines.

fig. 5 that this tendency is reversed and $m_R^c/\Delta\rho_{0R}$, $m_{0R}^c/\Delta\rho_{0R}$ start to decrease at about $\lambda_{1\Lambda} \simeq 2$.

In summary, the above results show that though the short distance potential U_Λ indicates a second order phase transition, the transition becomes first order once fluctuations are taken into account. This fluctuation induced first order phase transition is known in four dimensions as the Coleman-Weinberg phenomenon [31]. Previous studies of the three dimensional $U(2) \times U(2)$ symmetric model using the ϵ -expansion [32] already indicated that the phase transition should be a fluctuation induced first order transition. The validity of the ϵ -expansion for weak first order transitions is, however, not clear a priori since the expansion parameter is not small – there are known cases where it fails to predict correctly the order of the transition [33]. The question of the order of the phase transition has been addressed also in lattice studies [34] and in high-temperature expansion [35]. All studies are consistent with the first order nature of the transition and with the absence of nonperturbative infrared stable fixed points. It is, however, notoriously difficult to distinguish by these methods between weak first order and second order transitions. Our method gives here a clear and unambiguous answer and allows a detailed quantitative description of the phase transition. The universal form of the equation of state for weak first order phase transitions is presented in section 8.

In the following we specify the scale k_f for which we have given the effective average

$\lambda_{1\Lambda}$	$\lambda_{2\Lambda}$	$\frac{\Delta\rho_{0R}}{\Lambda}$	$\frac{m_R^c}{\Delta\rho_{0R}}$	$\frac{m_{0R}^c}{\Delta\rho_{0R}}$	$\lambda_{1\Lambda}$	$\lambda_{2\Lambda}$	$\frac{\Delta\rho_{0R}}{\Lambda}$	$\frac{m_R^c}{\Delta\rho_{0R}}$	$\frac{m_{0R}^c}{\Delta\rho_{0R}}$
0.1	0.005	0.386×10^{-6}	1.69	1.26	2	2	0.392×10^{-2}	1.66	1.24
0.1	0.01	0.158×10^{-5}	1.68	1.26	2	6	0.230×10^{-1}	1.68	1.25
0.1	0.05	0.461×10^{-4}	1.66	1.23	2	15	0.505×10^{-1}	1.80	1.35
0.1	0.1	0.249×10^{-3}	1.58	1.17	2	30	0.649×10^{-1}	1.91	1.45
0.1	0.2	0.193×10^{-2}	1.34	0.992	2	70	0.712×10^{-1}	2.01	1.60
0.1	0.5	0.316×10^{-1}	0.772	0.571	2	150	0.699×10^{-1}	2.02	1.65
0.1	1	0.145	0.527	0.395	2	350	0.685×10^{-1}	2.03	1.68
0.1	2	0.341	0.455	0.360	4	0.2	0.298×10^{-4}	1.69	1.26
0.1	5	0.547	0.450	0.414	4	2	0.213×10^{-2}	1.70	1.27
0.1	10	0.610	0.462	0.490	4	12	0.195×10^{-1}	1.80	1.35
2	0.02	0.523×10^{-6}	1.69	1.26	4	30	0.302×10^{-1}	1.89	1.43
2	0.1	0.121×10^{-4}	1.69	1.26	4	70	0.355×10^{-1}	1.96	1.49
2	0.3	0.101×10^{-3}	1.69	1.25	4	150	0.369×10^{-1}	1.98	1.55
2	1	0.104×10^{-2}	1.66	1.25	4	350	0.372×10^{-1}	1.97	1.57

Table 1: The discontinuity in the renormalized order parameter $\Delta\rho_{0R}$ and the critical inverse correlation lengths m_R^c and m_{0R}^c in the ordered and the disordered phase respectively. For small $\lambda_{2\Lambda}/\lambda_{1\Lambda}$ the ratios $m_R^c/\Delta\rho_{0R}$ and $m_{0R}^c/\Delta\rho_{0R}$ become universal.

potential U_k . We observe that U_k depends strongly on the infrared cutoff k as long as k is larger than the scale k_2 where the second minimum of the potential appears. Below k_2 the two minima start to become almost degenerate for T near T_c and the running of $\rho_0(k)$ stops rather soon. The nonvanishing value of k_2 induces a physical infrared cutoff and represents a characteristic scale for the first order phase transition. We stop the integration of the flow equation for the effective average potential at a scale $k_f < k_2$ which is determined in terms of the curvature (mass term) at the top of the potential barrier that separates the two local minima of U_k at the origin and at $\rho_0(k)$. The top of the potential barrier at $\rho_B(k)$ is determined by

$$U'_k(\rho_B) = 0 \quad (4.9)$$

for $0 < \rho_B(k) < \rho_0(k)$ and for the renormalized mass term at $\rho_B(k)$ one obtains

$$m_{B,R}^2(k) = 2Z_k^{-1}\rho_B U''_k(\rho_B) < 0. \quad (4.10)$$

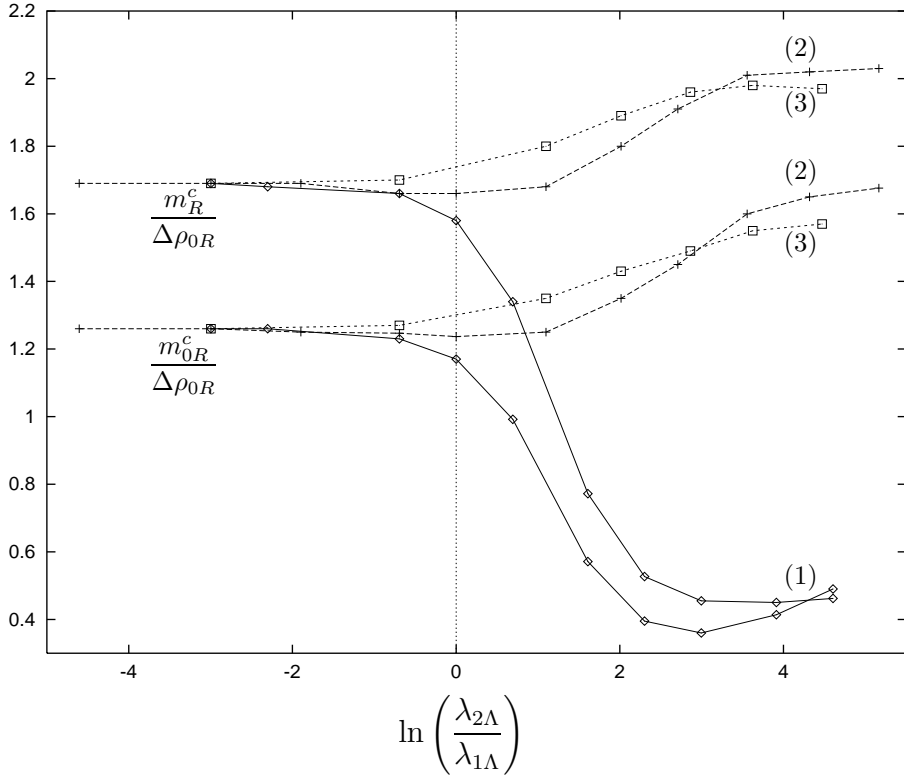


Figure 5: The inverse correlation lengths m_R^c and m_{0R}^c in the ordered and the disordered phase respectively. They are normalized to $\Delta\rho_{0R}$ and given as a function of $\ln(\lambda_{2\Lambda}/\lambda_{1\Lambda})$. Data points for fixed (1) $\lambda_{1\Lambda} = 0.1$, (2) $\lambda_{1\Lambda} = 2$, (3) $\lambda_{1\Lambda} = 4$ are connected by straight lines.

We fix our final value for the running by

$$\frac{k_f^2 - |m_{B,R}^2(k_f)|}{k_f^2} = 0.01 \quad (4.11)$$

For this choice the coarse grained effective potential U_{k_f} essentially includes all fluctuations with momenta larger than the mass $|m_{B,R}|$ at the top of the potential barrier. It is a nonconvex function which is the appropriate quantity for the study of physical processes such as tunneling or inflation. The nonconvex part of U_k is considered in detail in section 9. There we will also discuss that the appropriate choice for a coarse graining scale k is often far from obvious.

5 Scale dependence of the effective average potential

In this section we derive the flow equation for the effective average potential U_k . We point out a related investigation of the four dimensional $SU(N) \times SU(N)$ symmetric linear sigma model coupled to fermions that has been studied previously within the framework of the

effective average action [28]. There the flow equations for a polynomial approximation of U_k can be found for arbitrary dimension d . To study the equation of state of the three dimensional theory we keep here the most general form for U_k .

We define U_k by evaluating the average action for a constant field with $\Gamma_k = \Omega U_k$ where Ω denotes the volume. To evaluate the r.h.s. of (2.5) with the ansatz (3.2) we expand Γ_k around a constant background configuration. With the help of the $U(2) \times U(2)$ transformations the matrix field φ can be turned into a standard diagonal form with real nonnegative eigenvalues. Without loss of generality the evolution equation for the effective potential can therefore be obtained by calculating the trace in (2.5) for small field fluctuations χ_{ab} around a constant background configuration which is real and diagonal,

$$\varphi_{ab} = \varphi_a \delta_{ab} , \quad \varphi_a^* = \varphi_a . \quad (5.1)$$

We separate the fluctuation field into its real and imaginary part, $\chi_{ab} = \frac{1}{\sqrt{2}}(\chi_{Rab} + i\chi_{Iab})$ and perform the second functional derivatives of Γ_k with respect to the eight real components. For the constant configuration (5.1) it turns out that $\Gamma_k^{(2)}$ has a block diagonal form because mixed derivatives with respect to real and imaginary parts of the field vanish. The remaining submatrices $\delta^2\Gamma_k/\delta\chi_R^{ab}\delta\chi_R^{cd}$ and $\delta^2\Gamma_k/\delta\chi_I^{ab}\delta\chi_I^{cd}$ can be diagonalized in order to find the inverse of $\Gamma_k^{(2)} + R_k$ under the trace occurring in eq. (2.5). Here the momentum independent part of $\Gamma_k^{(2)}$ defines the mass matrix by the second functional derivatives of U_k . The eight eigenvalues of the mass matrix are

$$\begin{aligned} (M_1^\pm)^2 &= U'_k + 2(\rho \pm (\rho^2 - \tau)^{1/2}) \partial_\tau U_k , \\ (M_2^\pm)^2 &= U'_k \pm 2\tau^{1/2} \partial_\tau U_k \end{aligned} \quad (5.2)$$

corresponding to second derivatives with respect to χ_I and

$$\begin{aligned} (M_3^\pm)^2 &= (M_1^\pm)^2 , \\ (M_4^\pm)^2 &= U'_k + \rho U''_k + 2\rho \partial_\tau U_k + 4\tau \partial_\tau U'_k + 4\rho\tau \partial_\tau^2 U_k \\ &\quad \pm \left\{ \tau (U''_k + 4\partial_\tau U_k + 4\rho \partial_\tau U'_k + 4\tau \partial_\tau^2 U_k)^2 \right. \\ &\quad \left. + (\rho^2 - \tau) (U''_k - 2\partial_\tau U_k - 4\tau \partial_\tau^2 U_k)^2 \right\}^{1/2} \end{aligned} \quad (5.3)$$

corresponding to second derivatives with respect to χ_R . Here the eigenvalues are expressed in terms of the invariants ρ and τ using

$$\varphi_1^2 = \frac{1}{2}(\rho + \tau^{1/2}), \quad \varphi_2^2 = \frac{1}{2}(\rho - \tau^{1/2}) \quad (5.4)$$

and we adopt the convention that a prime on $U_k(\rho, \tau)$ denotes the derivative with respect to ρ at fixed τ and k and $\partial_\tau^n U_k \equiv \partial^n U_k / (\partial \tau)^n$.

The flow equation for the effective average potential is simply expressed in terms of

the mass eigenvalues

$$\begin{aligned} \frac{\partial}{\partial t} U_k(\rho, \tau) &= \frac{1}{2} \int \frac{d^d q}{(2\pi)^d} \frac{\partial}{\partial t} R_k(q) \\ &\left\{ \frac{2}{P_k(q) + (M_1^+(\rho, \tau))^2} + \frac{2}{P_k(q) + (M_1^-(\rho, \tau))^2} + \frac{1}{P_k(q) + (M_2^+(\rho, \tau))^2} \right. \\ &\left. + \frac{1}{P_k(q) + (M_2^-(\rho, \tau))^2} + \frac{1}{P_k(q) + (M_4^+(\rho, \tau))^2} + \frac{1}{P_k(q) + (M_4^-(\rho, \tau))^2} \right\}. \end{aligned} \quad (5.5)$$

On the right hand side of the evolution equation appears the (massless) inverse average propagator

$$P_k(q) = Z_k q^2 + R_k(q) = \frac{Z_k q^2}{1 - e^{-q^2/k^2}} \quad (5.6)$$

which incorporates the infrared cutoff function R_k given by eq. (2.3). The only approximation so far is due to the derivative expansion (3.2) of Γ_k which enters into the flow equation (5.5) through the form of P_k . The mass eigenvalues (5.2) and (5.3) appearing in the above flow equation are exact since we have kept for the potential the most general form $U_k(\rho, \tau)$.

Spontaneous symmetry breaking and mass spectra

In the following we consider spontaneous symmetry breaking patterns and the corresponding mass spectra for a few special cases. For the origin at $\varphi_{ab} = 0$ all eigenvalues equal $U'_k(0, 0)$. If the origin is the absolute minimum of the potential we are in the symmetric regime where all excitations have mass squared $U'_k(0, 0)$.

Spontaneous symmetry breaking to the diagonal $U(2)$ subgroup of $U(2) \times U(2)$ can be observed for a field configuration which is proportional to the identity matrix, i.e. $\varphi_{ab} = \varphi \delta_{ab}$. The invariants (3.3) take on values $\rho = 2\varphi^2$ and $\tau = 0$. The relevant information for this symmetry breaking pattern is contained in $U_k(\rho) \equiv U_k(\rho, \tau = 0)$. In case of spontaneous symmetry breaking there is a nonvanishing value for the minimum ρ_0 of the potential. With $U'_k(\rho_0) = 0$ one finds the expected four massless Goldstone bosons with $(M_1^-)^2 = (M_2^\pm)^2 = (M_3^-)^2 = 0$. In addition there are three massive scalars in the adjoint representation of the unbroken diagonal $SU(2)$ with mass squared $(M_1^+)^2 = (M_3^+)^2 = (M_4^-)^2 = 4\rho_0 \partial_\tau U_k$ and one singlet with mass squared $(M_4^+)^2 = 2\rho_0 U''_k$. The situation corresponds to chiral symmetry breaking in two flavor QCD in absence of quark masses and the chiral anomaly. The Goldstone modes are the pseudoscalar pions and the η (or η'), the scalar triplet has the quantum numbers of a_0 and the singlet is the so-called σ -field.

Another interesting case is the spontaneous symmetry breaking down to a residual $U(1) \times U(1) \times U(1)$ subgroup of $U(2) \times U(2)$ which can be observed for the configuration $\varphi_{ab} = \varphi \delta_{a1} \delta_{ab}$ ($\rho = \varphi^2$, $\tau = \varphi^4 = \rho^2$). Corresponding to the number of broken generators one observes the five massless Goldstone bosons $(M_1^\pm)^2 = (M_2^+)^2 = (M_3^\pm)^2 = 0$ for the minimum of the potential at $U'_k + 2\rho_0 \partial_\tau U_k = 0$. In addition there are two scalars with mass squared $(M_2^-)^2 = (M_4^-)^2 = U'_k - 2\rho_0 \partial_\tau U_k$ and one with $(M_4^+)^2 = U'_k + 2\rho_0 U''_k + 6\rho_0 \partial_\tau U_k + 8\rho_0^2 \partial_\tau U'_k + 8\rho_0^3 \partial_\tau^2 U_k$.

We finally point out the special case where the potential is independent of the second invariant τ . In this case there is an enhanced $O(8)$ symmetry instead of $U(2) \times U(2)$. With $\partial_\tau^n U_k \equiv 0$ and $U'_k(\rho_0) = 0$ one observes the expected seven massless Goldstone bosons and one massive mode with mass squared $2\rho_0 U''_k$.

Scaling form of the flow equation

For the $O(8)$ symmetric model in the limit $\bar{\lambda}_{2\Lambda} = 0$ one expects a region of the parameter space which is characterized by renormalized masses much smaller than the ultraviolet cutoff or inverse microscopic length scale of the theory. In particular, in the absence of a mass scale one expects a scaling behavior of the effective average potential U_k . The behavior of U_k at or near a second order phase transition is most conveniently studied using the scaling form of the evolution equation. This form is also appropriate for an investigation that has to deal with weak first order phase transitions as encountered in the present model for $\bar{\lambda}_{2\Lambda} > 0$. The remaining part of this section is devoted to the derivation of the scaling form (5.15) of the flow equation (5.5).

In the present form of eq. (5.5) the r.h.s. shows an explicit dependence on the scale k once the momentum integration is performed. By a proper choice of variables we cast the evolution equation into a form where the scale no longer appears explicitly. We introduce a dimensionless potential $u_k = k^{-d} U_k$ and express it in terms of dimensionless renormalized fields

$$\begin{aligned}\tilde{\rho} &= Z_k k^{2-d} \rho, \\ \tilde{\tau} &= Z_k^2 k^{4-2d} \tau.\end{aligned}\tag{5.7}$$

The derivatives of u_k are given by

$$\partial_{\tilde{\tau}}^n u_k^{(m)}(\tilde{\rho}, \tilde{\tau}) = Z_k^{-2n-m} k^{(2n+m-1)d-4n-2m} \partial_\tau^n U_k^{(m)}(\rho, \tau).\tag{5.8}$$

(Note that $u_k^{(m)}$ denotes m derivatives with respect to $\tilde{\rho}$ at fixed $\tilde{\tau}$ and k , while $U_k^{(m)}$ denotes m derivatives with respect to ρ at fixed τ and k). With

$$\begin{aligned}\frac{\partial}{\partial t} u_k(\tilde{\rho}, \tilde{\tau})|_{\tilde{\rho}, \tilde{\tau}} &= -du_k(\tilde{\rho}, \tilde{\tau}) + (d-2+\eta)\tilde{\rho} u'_k(\tilde{\rho}, \tilde{\tau}) + (2d-4+2\eta)\tilde{\tau} \partial_{\tilde{\tau}} u_k(\tilde{\rho}, \tilde{\tau}) \\ &\quad + k^{-d} \frac{\partial}{\partial t} U_k(\rho(\tilde{\rho}), \tau(\tilde{\tau}))|_{\rho, \tau}\end{aligned}\tag{5.9}$$

one obtains from (5.5) the evolution equation for the dimensionless potential. Here the anomalous dimension η arises from the t -derivative acting on Z_k and is given by eq. (3.5). It is convenient to introduce dimensionless integrals by

$$\frac{1}{2} \int \frac{d^d q}{(2\pi)^d} \frac{\partial R_k}{\partial t} \frac{1}{P_k + Z_k k^2 \omega} = 2v_d k^d [I_0^d(\omega) - \eta \hat{I}_0^d(\omega)]\tag{5.10}$$

where

$$v_d^{-1} = 2^{d+1} \pi^{\frac{d}{2}} \Gamma\left(\frac{d}{2}\right).\tag{5.11}$$

The explicit form of l_0^d and \hat{l}_0^d reads

$$\begin{aligned} l_0^d(\omega) &= - \int_0^\infty dy y^{\frac{d}{2}+1} \frac{\partial r(y)}{\partial y} [y(1+r(y)) + \omega]^{-1}, \\ \hat{l}_0^d(\omega) &= \frac{1}{2} \int_0^\infty dy y^{\frac{d}{2}} r(y) [y(1+r(y)) + \omega]^{-1} \end{aligned} \quad (5.12)$$

with the dimensionless infrared cutoff function

$$r(y) = \frac{e^{-y}}{1 - e^{-y}}. \quad (5.13)$$

The behavior of these functions is discussed in section 6 where we also consider their derivatives with respect to ω . Using the notation

$$l_0^d(\omega; \eta) = l_0^d(\omega) - \eta \hat{l}_0^d(\omega) \quad (5.14)$$

one obtains the flow equation for the dimensionless potential

$$\begin{aligned} \frac{\partial}{\partial t} u_k(\tilde{\rho}, \tilde{\tau}) &= -du_k(\tilde{\rho}, \tilde{\tau}) + (d-2+\eta)\tilde{\rho}u'_k(\tilde{\rho}, \tilde{\tau}) + (2d-4+2\eta)\tilde{\tau}\partial_{\tilde{\tau}}u_k(\tilde{\rho}, \tilde{\tau}) \\ &+ 4v_d l_0^d((m_1^+(\tilde{\rho}, \tilde{\tau}))^2; \eta) + 4v_d l_0^d((m_1^-(\tilde{\rho}, \tilde{\tau}))^2; \eta) + 2v_d l_0^d((m_2^+(\tilde{\rho}, \tilde{\tau}))^2; \eta) \\ &+ 2v_d l_0^d((m_2^-(\tilde{\rho}, \tilde{\tau}))^2; \eta) + 2v_d l_0^d((m_3^+(\tilde{\rho}, \tilde{\tau}))^2; \eta) + 2v_d l_0^d((m_3^-(\tilde{\rho}, \tilde{\tau}))^2; \eta) \end{aligned} \quad (5.15)$$

where the dimensionless mass terms are related to (5.3) according to

$$(m_i^\pm(\tilde{\rho}, \tilde{\tau}))^2 = \frac{(M_i^\pm(\rho(\tilde{\rho}), \tau(\tilde{\tau})))^2}{Z_k k^2}. \quad (5.16)$$

Eq. (5.15) is the scaling form of the flow equation we are looking for. For a $\tilde{\tau}$ -independent potential it reduces to the evolution equation for the $O(8)$ symmetric model [27, 22]. The potential u_k at a second order phase transition is given by a k -independent (scaling) solution $\partial u_k / \partial t = 0$ [27, 22]. For this solution all the k -dependent functions on the r.h.s. of eq. (5.15) become independent of k . For a weak first order phase transition these functions will show a weak k -dependence for k larger than the inherent mass scale of the system (cf. section 7). There is no particular advantage of the scaling form of the flow equation for strong first order phase transitions.

6 Solving the flow equation

Eq. (5.15) describes the scale dependence of the effective average potential u_k by a non-linear partial differential equation for the three variables t , $\tilde{\rho}$ and $\tilde{\tau}$. A major difficulty for its analytical study is that the integral $l_0^d(\omega; \eta)$ (cf. eq. (5.12)) can be done analytically

only for certain limits of the arguments. The complicated form of the equation therefore suggests a numerical solution. We will use a method that relies on a simultaneous expansion of the potential around a number of field values $\tilde{\rho}_i, \tilde{\tau}_j$, $i = 1, \dots, l$, $j = 1, \dots, l'$ for given numbers l, l' . The expansions around different points are matched to obtain the general field dependence of the potential. As a consequence we cast the partial differential equation (5.15) into a system of ordinary differential equations. The method is developed in [37] for a computation of the critical equation of state for $O(N)$ symmetric models [15]. The generalization to the present model is described below. This approach has some favorable aspects. The main advantage is that it allows the integration of the differential equations using a standard Runge-Kutta algorithm without the occurrence of numerical instabilities. (See e.g. [37] for instability problems with standard discretised versions of partial differential equations in the context of flow equations). The coupled set of ordinary differential equations describes the flow of couplings defined as derivatives of the potential at given points, e.g. at the minimum of the potential. These couplings often allow direct physical interpretation and some of their properties can be read off from the analytic structure of their flow equations. We will exploit this fact to explain the results we obtain from the numerical solution in section 7.

We concentrate in the following on spontaneous symmetry breaking with a residual $U(2)$ symmetry group. As we have already pointed out in section 3 this symmetry breaking can be observed for a configuration which is proportional to the identity and we have $\tilde{\tau} = 0$. In this case the eigenvalues (5.2) and (5.3) of the mass matrix with (5.16) are given by

$$\begin{aligned} (m_1^-)^2 &= (m_2^\pm)^2 = (m_3^-)^2 = u'_k, \\ (m_1^+)^2 &= (m_3^+)^2 = (m_4^-)^2 = u'_k + 4\tilde{\rho}\partial_{\tilde{\tau}}u_k, \\ (m_4^+)^2 &= u'_k + 2\tilde{\rho}u''_k \end{aligned} \tag{6.1}$$

and on the r.h.s. of the partial differential equation (5.15) for $u_k(\tilde{\rho}) \equiv u_k(\tilde{\rho}, \tilde{\tau} = 0)$ only the functions $u'_k(\tilde{\rho})$, $u''_k(\tilde{\rho})$ and $\partial_{\tilde{\tau}}u_k(\tilde{\rho})$ appear. At fixed $\tilde{\rho} = \tilde{\rho}_i$ the k -dependence of u_k is then determined by the couplings $u'_k(\tilde{\rho}_i)$, $u''_k(\tilde{\rho}_i)$ and $\partial_{\tilde{\tau}}u_k(\tilde{\rho}_i)$. We determine these couplings through the use of flow equations which are obtained by taking the derivative in eq. (5.15) with respect to $\tilde{\rho}$ and $\tilde{\tau}$ evaluated at $\tilde{\rho} = \tilde{\rho}_i$, $\tilde{\tau} = 0$. These flow equations for u'_k , u''_k and $\partial_{\tilde{\tau}}u_k$ involve also higher derivatives of the potential as u'''_k , $u_k^{(4)}$, $\partial_{\tilde{\tau}}u'_k$ and $\partial_{\tilde{\tau}}u''_k$. The procedure will be to evaluate the flow equations for u'_k and u''_k at different points $\tilde{\rho}_i, \tilde{\tau} = 0$ for $i = 1, \dots, l$ and to estimate the higher $\tilde{\rho}$ -derivatives appearing on the right hand side of the flow equations by imposing matching conditions. The same procedure can be applied to $\partial_{\tilde{\tau}}u_k$ and in order to obtain an equivalent matching we also consider the flow equation for $\partial_{\tilde{\tau}}u'_k$. One could proceed in a similar way for $\partial_{\tilde{\tau}}^2u_k$ which appears on the right hand side of the evolution equation of $\partial_{\tilde{\tau}}u_k$ and so on. However, since we are interested in the $\tilde{\rho}$ -dependence of the potential at $\tilde{\tau} = 0$ we shall use a truncated expansion⁴ in $\tilde{\tau}$ with

$$\partial_{\tilde{\tau}}^n u_k(\tilde{\rho}, \tilde{\tau} = 0) = 0 \quad \text{for } n \geq 2. \tag{6.2}$$

⁴In principle one could also consider points with $\tilde{\tau} \neq 0$ in the neighborhood of $\tilde{\tau} = 0$ and use the additional information to estimate the higher $\tilde{\tau}$ -derivatives as it is done for the higher $\tilde{\rho}$ -derivatives.

In three space dimensions the neglected ($\tilde{\rho}$ -dependent) operators have negative canonical mass dimension. We make no expansion in terms of $\tilde{\rho}$ since the general $\tilde{\rho}$ -dependence allows a description of a first order phase transition where a second local minimum of $u_k(\tilde{\rho})$ appears. The approximation (6.2) only affects the flow equations for $\partial_{\tilde{\tau}}u_k$ and $\partial_{\tilde{\tau}}u'_k$ (cf. eqs. (6.9) and (6.10)). The form of the flow equations for u'_k and u''_k is not affected by the truncation (cf. eqs. (6.7) and (6.8)). From u'_k we obtain the effective average potential u_k by simple integration. We have tested the sensitivity of our results for u'_k to a change in $\partial_{\tilde{\tau}}u_k$ by neglecting the $\tilde{\rho}$ -dependence of the $\tilde{\tau}$ -derivative. We observed no qualitative change of the results. We expect that the main truncation error is due to the derivative expansion (3.2) for the effective average action.

To simplify notation we introduce

$$\begin{aligned}\epsilon(\tilde{\rho}) &= u'_k(\tilde{\rho}, \tilde{\tau} = 0), \\ \lambda_1(\tilde{\rho}) &= u''_k(\tilde{\rho}, \tilde{\tau} = 0), \\ \lambda_2(\tilde{\rho}) &= 4\partial_{\tilde{\tau}}u_k(\tilde{\rho}, \tilde{\tau} = 0).\end{aligned}\tag{6.3}$$

Higher derivatives are denoted by primes on the $\tilde{\rho}$ -dependent quartic 'couplings', i.e. $\lambda'_1 = u'''_k$, $\lambda'_2 = \partial_{\tilde{\tau}}u'_k$ etc. It is convenient to introduce functions $l_n^d(\omega; \eta)$ that can be related to $l_0^d(\omega; \eta)$ (5.12) by differentiation with respect to the mass argument:

$$\begin{aligned}l_1^d(\omega; \eta) &= l_1^d(\omega) - \eta \hat{l}_1^d(\omega) \\ &= -\frac{\partial}{\partial \omega} l_0^d(\omega; \eta), \\ l_{n+1}^d(\omega; \eta) &= -\frac{1}{n} \frac{\partial}{\partial \omega} l_n^d(\omega; \eta) \quad \text{for } n \geq 1.\end{aligned}\tag{6.4}$$

The explicit form of l_n^d and \hat{l}_n^d is given in eq. (A.1) in the appendix. For $\omega \geq -1$ they are positive, monotonically decreasing functions of ω . In leading order l_n^d and \hat{l}_n^d vanish $\sim \omega^{-(n+1)}$ for arguments $\omega \gg 1$. They introduce a 'threshold' behavior that accounts for the decoupling of modes with mass squared larger than the infrared cutoff $Z_k k^2$. For vanishing argument they are of order unity. As $\omega \rightarrow -1$ the functions l_n^d , \hat{l}_n^d exhibit a pole for $d < 2(n+1)$. The pole structure is discussed in the appendix. We also use two-parameter functions $l_{n_1, n_2}^d(\omega_1, \omega_2; \eta)$ [28]. For $n_1 = n_2 = 1$ their relation to the functions $l_n^d(\omega; \eta)$ can be expressed as

$$\begin{aligned}l_{1,1}^d(\omega_1, \omega_2; \eta) &= \frac{1}{\omega_2 - \omega_1} [l_1^d(\omega_1; \eta) - l_1^d(\omega_2; \eta)] \quad \text{for } \omega_1 \neq \omega_2, \\ l_{1,1}^d(\omega, \omega; \eta) &= l_2^d(\omega; \eta)\end{aligned}\tag{6.5}$$

and

$$l_{n_1+1, n_2}^d(\omega_1, \omega_2; \eta) = -\frac{1}{n_1} \frac{\partial}{\partial \omega_1} l_{n_1, n_2}^d(\omega_1, \omega_2; \eta), \quad l_{n_1, n_2}^d(\omega_1, \omega_2; \eta) = l_{n_2, n_1}^d(\omega_2, \omega_1; \eta).\tag{6.6}$$

With the help of these functions the scale dependence of ϵ is described by

$$\begin{aligned} \frac{\partial \epsilon}{\partial t} = & (-2 + \eta)\epsilon + (d - 2 + \eta)\tilde{\rho}\lambda_1 - 6v_d(\lambda_1 + \lambda_2 + \tilde{\rho}\lambda'_2)l_1^d(\epsilon + \tilde{\rho}\lambda_2; \eta) \\ & - 2v_d(3\lambda_1 + 2\tilde{\rho}\lambda'_1)l_1^d(\epsilon + 2\tilde{\rho}\lambda_1; \eta) - 8v_d\lambda_1 l_1^d(\epsilon; \eta) \end{aligned} \quad (6.7)$$

and for λ_1 one finds

$$\begin{aligned} \frac{\partial \lambda_1}{\partial t} = & (d - 4 + 2\eta)\lambda_1 + (d - 2 + \eta)\tilde{\rho}\lambda'_1 \\ & + 6v_d \left[(\lambda_1 + \lambda_2 + \tilde{\rho}\lambda'_2)^2 l_2^d(\epsilon + \tilde{\rho}\lambda_2; \eta) - (\lambda'_1 + 2\lambda'_2 + \tilde{\rho}\lambda''_2) l_1^d(\epsilon + \tilde{\rho}\lambda_2; \eta) \right] \\ & + 2v_d \left[(3\lambda_1 + 2\tilde{\rho}\lambda'_1)^2 l_2^d(\epsilon + 2\tilde{\rho}\lambda_1; \eta) - (5\lambda'_1 + 2\tilde{\rho}\lambda''_1) l_1^d(\epsilon + 2\tilde{\rho}\lambda_1; \eta) \right] \\ & + 8v_d \left[(\lambda_1)^2 l_2^d(\epsilon; \eta) - \lambda'_1 l_1^d(\epsilon; \eta) \right]. \end{aligned} \quad (6.8)$$

Similarly the scale dependence of λ_2 is given by

$$\begin{aligned} \frac{\partial \lambda_2}{\partial t} = & (d - 4 + 2\eta)\lambda_2 + (d - 2 + \eta)\tilde{\rho}\lambda'_2 - 4v_d(\lambda_2)^2 l_{1,1}^d(\epsilon + \tilde{\rho}\lambda_2, \epsilon; \eta) \\ & + 2v_d \left[3(\lambda_2)^2 + 12\lambda_1\lambda_2 + 8\tilde{\rho}\lambda'_2(\lambda_1 + \lambda_2) + 4\tilde{\rho}^2(\lambda'_2)^2 \right] l_{1,1}^d(\epsilon + \tilde{\rho}\lambda_2, \epsilon + 2\tilde{\rho}\lambda_1; \eta) \\ & - 14v_d\lambda'_2 l_1^d(\epsilon + \tilde{\rho}\lambda_2; \eta) - 2v_d(5\lambda'_2 + 2\tilde{\rho}\lambda''_2) l_1^d(\epsilon + 2\tilde{\rho}\lambda_1; \eta) \\ & + 2v_d \left[(\lambda_2)^2 l_2^d(\epsilon; \eta) - 4\lambda'_2 l_1^d(\epsilon; \eta) \right] \end{aligned} \quad (6.9)$$

and for λ'_2 it reads

$$\begin{aligned} \frac{\partial \lambda'_2}{\partial t} = & (2d - 6 + 3\eta)\lambda'_2 + (d - 2 + \eta)\tilde{\rho}\lambda''_2 \\ & + 4v_d(\lambda_2)^2 \left[(\lambda_1 + \lambda_2 + \tilde{\rho}\lambda'_2) l_{2,1}^d(\epsilon + \tilde{\rho}\lambda_2, \epsilon; \eta) + \lambda_1 l_{1,2}^d(\epsilon + \tilde{\rho}\lambda_2, \epsilon; \eta) \right] \\ & - 2v_d \left[3\lambda_2(4\lambda_1 + \lambda_2) + 4\tilde{\rho}\lambda'_2(2\lambda_1 + 2\lambda_2 + \tilde{\rho}\lambda'_2) \right] \left[(\lambda_1 + \lambda_2 + \tilde{\rho}\lambda'_2) \right. \\ & \left. l_{2,1}^d(\epsilon + \tilde{\rho}\lambda_2, \epsilon + 2\tilde{\rho}\lambda_1; \eta) + (3\lambda_1 + 2\tilde{\rho}\lambda'_1) l_{1,2}^d(\epsilon + \tilde{\rho}\lambda_2, \epsilon + 2\tilde{\rho}\lambda_1; \eta) \right] \\ & + 4v_d \left[\lambda'_2(7\lambda_2 + 10\lambda_1) + 6\lambda_2\lambda'_1 + 4\tilde{\rho}(\lambda''_2(\lambda_1 + \lambda_2 + \tilde{\rho}\lambda'_2) + \lambda'_2(2\lambda'_2 + \lambda'_1)) \right] \\ & \left. l_{1,1}^d(\epsilon + \tilde{\rho}\lambda_2, \epsilon + 2\tilde{\rho}\lambda_1; \eta) - 8v_d\lambda_2\lambda'_2 l_{1,1}^d(\epsilon + \tilde{\rho}\lambda_2, \epsilon; \eta) \right. \\ & \left. + 2v_d(3\lambda_1 + 2\tilde{\rho}\lambda'_1)(5\lambda'_2 + 2\tilde{\rho}\lambda''_2) l_2^d(\epsilon + 2\tilde{\rho}\lambda_1; \eta) + 14v_d\lambda'_2(\lambda_1 + \lambda_2 + \tilde{\rho}\lambda'_2) \right. \\ & \left. l_2^d(\epsilon + \tilde{\rho}\lambda_2; \eta) - 2v_d(7\lambda''_2 + 2\tilde{\rho}\lambda'''_2) l_1^d(\epsilon + 2\tilde{\rho}\lambda_1; \eta) - 14v_d\lambda''_2 l_1^d(\epsilon + \tilde{\rho}\lambda_2; \eta) \right. \\ & \left. - 4v_d(\lambda_2)^2 \lambda_1 l_3^d(\epsilon; \eta) + 4v_d\lambda'_2(2\lambda_1 + \lambda_2) l_2^d(\epsilon; \eta) - 8v_d\lambda''_2 l_1^d(\epsilon; \eta) \right]. \end{aligned} \quad (6.10)$$

We evaluate the above flow equations at different points $\tilde{\rho}_i$ for $i = 1, \dots, l$ and use a set of matching conditions that has been proposed in ref. [37]. The generalization of

these conditions to the present model is obtained by considering fourth order polynomial expansions of $\epsilon(\tilde{\rho})$ and $\lambda_2(\tilde{\rho})$ around some arbitrary point $\tilde{\rho}_i$,

$$\begin{aligned}(\epsilon)_i(\tilde{\rho}) &= \epsilon_i + \lambda_{1,i}(\tilde{\rho} - \tilde{\rho}_i) + \frac{1}{2}\lambda'_{1,i}(\tilde{\rho} - \tilde{\rho}_i)^2 + \frac{1}{6}\lambda''_{1,i}(\tilde{\rho} - \tilde{\rho}_i)^3, \\(\lambda_2)_i(\tilde{\rho}) &= \lambda_{2,i} + \lambda'_{2,i}(\tilde{\rho} - \tilde{\rho}_i) + \frac{1}{2}\lambda''_{2,i}(\tilde{\rho} - \tilde{\rho}_i)^2 + \frac{1}{6}\lambda'''_{2,i}(\tilde{\rho} - \tilde{\rho}_i)^3\end{aligned}\tag{6.11}$$

with $\epsilon_i = \epsilon(\tilde{\rho}_i)$, $\lambda_{2,i} = \lambda_2(\tilde{\rho}_i)$ etc. Using similar expressions for

$$(\lambda_1)_i(\tilde{\rho}) = \frac{\partial}{\partial \tilde{\rho}}(\epsilon)_i(\tilde{\rho}) \quad , \quad (\lambda'_2)_i(\tilde{\rho}) = \frac{\partial}{\partial \tilde{\rho}}(\lambda_2)_i(\tilde{\rho})\tag{6.12}$$

the matching is done by imposing continuity at half distance between neighboring expansion points,

$$\begin{aligned}(\epsilon)_i\left(\frac{\tilde{\rho}_i + \tilde{\rho}_{i+1}}{2}\right) &= (\epsilon)_{i+1}\left(\frac{\tilde{\rho}_i + \tilde{\rho}_{i+1}}{2}\right) \quad , \quad (\lambda_1)_i\left(\frac{\tilde{\rho}_i + \tilde{\rho}_{i+1}}{2}\right) = (\lambda_1)_{i+1}\left(\frac{\tilde{\rho}_i + \tilde{\rho}_{i+1}}{2}\right), \\(\lambda_2)_i\left(\frac{\tilde{\rho}_i + \tilde{\rho}_{i+1}}{2}\right) &= (\lambda_2)_{i+1}\left(\frac{\tilde{\rho}_i + \tilde{\rho}_{i+1}}{2}\right) \quad , \quad (\lambda'_2)_i\left(\frac{\tilde{\rho}_i + \tilde{\rho}_{i+1}}{2}\right) = (\lambda'_2)_{i+1}\left(\frac{\tilde{\rho}_i + \tilde{\rho}_{i+1}}{2}\right)\end{aligned}\tag{6.13}$$

for $i = 1, \dots, l-1$ and

$$(\lambda'_1)_j\left(\frac{\tilde{\rho}_j + \tilde{\rho}_{j+1}}{2}\right) = (\lambda'_1)_{j+1}\left(\frac{\tilde{\rho}_j + \tilde{\rho}_{j+1}}{2}\right) \quad , \quad (\lambda''_2)_j\left(\frac{\tilde{\rho}_j + \tilde{\rho}_{j+1}}{2}\right) = (\lambda''_2)_{j+1}\left(\frac{\tilde{\rho}_j + \tilde{\rho}_{j+1}}{2}\right)\tag{6.14}$$

for the initial and end points, $j = 1$ and $j = l-1$. Together these $4(l-1)$ conditions (6.13) for all $l-1 \geq 2$ intermediate points and the four conditions (6.14) make up two independent algebraic systems of each $2l$ equations. From the first set of equations one obtains a unique solution for $\lambda'_{1,i}$ and $\lambda''_{1,i}$. The second set is identical in structure and $\lambda''_{2,i}$, $\lambda'''_{2,i}$ can be obtained from the solutions for $\lambda'_{1,i}$ and $\lambda''_{1,i}$ with the substitutions $\epsilon_j \rightarrow \lambda_{2,j}$, $\lambda_{1,j} \rightarrow \lambda'_{2,j}$, $\lambda'_{1,j} \rightarrow \lambda''_{2,j}$, $\lambda''_{1,j} \rightarrow \lambda'''_{2,j}$ for $j = 1, \dots, l$. With the help of these algebraic solutions we eliminate $\lambda'_1(\tilde{\rho})$, $\lambda''_1(\tilde{\rho})$, $\lambda''_2(\tilde{\rho})$ and $\lambda'''_2(\tilde{\rho})$ in the flow equations (6.7) - (6.10) for all l points $\tilde{\rho}_i$.⁵ Therefore, equations (6.7) - (6.10) are turned into a closed system of

⁵The algebraic solutions $\lambda'_{1,i}$ and $\lambda''_{1,i}$ (equivalently $\lambda''_{2,i}$ and $\lambda'''_{2,i}$) do incorporate information from the whole range of points $\tilde{\rho}_j$ with $j = 1, \dots, l$. It is a feature of the matching conditions (6.13), (6.14) that the contributions from points $\tilde{\rho}_{j \neq i}$ to $\lambda'_{1,i}$, $\lambda''_{1,i}$ rapidly decrease with increasing $|i-j|$. For equal spacings between neighboring expansion points contributions from points $\tilde{\rho}_j$ with $j > i+1$ ($j < i-1$) are typically suppressed by a factor $\lesssim 10^{-|i-j|+1}$ as compared to the contribution from the nearest neighbor point $\tilde{\rho}_{i+1}$ ($\tilde{\rho}_{i-1}$). As a consequence solutions $\lambda'_{1,i}$, $\lambda''_{1,i}$ for inner points with $1 \ll i \ll l$ become independent from boundary points. We observe approximate translational invariance for inner point solutions, i.e. $\lambda'_{1,i \pm n}$ and $\lambda''_{1,i \pm n}$ are approximately obtained from the solutions $\lambda'_{1,i}$ and $\lambda''_{1,i}$ with the substitutions $\epsilon_j \rightarrow \epsilon_{j \pm n}$, $\lambda_{1,j} \rightarrow \lambda_{1,j \pm n}$ for $1 \leq j \leq l$ if i and $i \pm n$ are sufficiently far away from the boundaries. The decoupling from distant points and the translational invariance for inner points can be used to obtain approximate expressions which become useful if a large number of expansion points is considered. We use the exact algebraic solution for $l = 10$ points. For $l > 10$ we apply the approximate translational invariance to generate from $\lambda'_{1,5}$, $\lambda'_{1,6}$ additional solutions $\lambda'_{1,5+2i}$, $\lambda'_{1,6+2i}$ for $i = 1, \dots, (l-10)/2$ with l even and equivalently for $\lambda''_{1,5}$, $\lambda''_{1,6}$. With $\lambda'_{1,l-3}, \dots, \lambda'_{1,l}$ and $\lambda''_{1,l-3}, \dots, \lambda''_{1,l}$ from the calculation with 10 points one obtains the desired generalization. We have used runs with different choices of l in order to check the stability of the numerical results.

$4l$ ordinary differential equations for the unknowns $\epsilon(\tilde{\rho}_i)$, $\lambda_1(\tilde{\rho}_i)$, $\lambda_2(\tilde{\rho}_i)$ and $\lambda_2'(\tilde{\rho}_i)$.

If there is a minimum of the potential at nonvanishing $\kappa \equiv \tilde{\rho}_0$ we use expansion points that are proportional to the minimum, i.e. $\tilde{\rho}_i = \frac{i-1}{n}\kappa$ with $i = 1, \dots, l$ and fixed integer n . The condition $\epsilon(\kappa) = 0$ can be used to obtain the scale dependence of $\kappa(k)$:

$$\begin{aligned} \frac{d\kappa}{dt} &= -[\lambda_1(\kappa)]^{-1} \frac{\partial \epsilon}{\partial t} \Big|_{\tilde{\rho}=\kappa} \\ &= -(d-2+\eta)\kappa + 6v_d \left(1 + \frac{\lambda_2(\kappa) + \kappa \lambda_2'(\kappa)}{\lambda_1(\kappa)} \right) l_1^d(\kappa \lambda_2(\kappa); \eta) \\ &\quad + 2v_d \left(3 + \frac{2\kappa \lambda_1'(\kappa)}{\lambda_1(\kappa)} \right) l_1^d(2\kappa \lambda_1(\kappa); \eta) + 8v_d l_1^d(0; \eta). \end{aligned} \quad (6.15)$$

To make contact with β -functions for the couplings at the potential minimum κ we point out the relation

$$\frac{d\lambda_{1,2}^{(m)}(\kappa)}{dt} = \frac{\partial \lambda_{1,2}^{(m)}}{\partial t} \Big|_{\tilde{\rho}=\kappa} + \lambda_{1,2}^{(m+1)}(\kappa) \frac{d\kappa}{dt}. \quad (6.16)$$

Similar relations hold for $\epsilon(\tilde{\rho}_i)$, $\lambda_1(\tilde{\rho}_i)$ etc., e.g.

$$\begin{aligned} \frac{d\epsilon(\tilde{\rho}_i)}{dt} &= \frac{\partial \epsilon}{\partial t} \Big|_{\tilde{\rho}=\tilde{\rho}_i} + \frac{i-1}{n} \lambda_1(\tilde{\rho}_i) \frac{d\kappa}{dt}, \\ \frac{d\lambda_1(\tilde{\rho}_i)}{dt} &= \frac{\partial \lambda_1}{\partial t} \Big|_{\tilde{\rho}=\tilde{\rho}_i} + \frac{i-1}{n} \lambda_1'(\tilde{\rho}_i) \frac{d\kappa}{dt}. \end{aligned} \quad (6.17)$$

We integrate the $4l-1$ differential equations (6.7) - (6.10) for the couplings $\epsilon(\tilde{\rho}_i)$, $\lambda_1(\tilde{\rho}_i)$, $\lambda_2(\tilde{\rho}_i)$ and $\lambda_2'(\tilde{\rho}_i)$ (with $\partial/\partial t$ replaced by d/dt according to (6.17)) and the one for κ (6.15) with a fifth-order Runge-Kutta algorithm using the embedded fourth-order method for precision control. The general $\tilde{\rho}$ -dependence is recovered by patching the simultaneous expansions around different points at half distance between neighboring expansion points.

It remains to compute the anomalous dimension η defined in (3.5) which describes the scale dependence of the wave function renormalization Z_k . We consider a space dependent distortion of the constant background field configuration (5.1) of the form

$$\varphi_{ab}(x) = \varphi_a \delta_{ab} + \left[\delta\varphi e^{-iQx} + \delta\varphi^* e^{iQx} \right] \Sigma_{ab}. \quad (6.18)$$

Insertion of the above configuration into the parametrization (3.2) of Γ_k yields

$$Z_k = Z_k(\rho, \tau, Q^2 = 0) = \frac{1}{2} \frac{1}{\Sigma_{ab}^* \Sigma_{ab}} \lim_{Q^2 \rightarrow 0} \frac{\partial}{\partial Q^2} \frac{\delta \Gamma_k}{\delta(\delta\varphi \delta\varphi^*)} \Big|_{\delta\varphi=0}. \quad (6.19)$$

To obtain the flow equation of the wave function renormalization one expands the effective average action around a configuration of the form (6.18) and evaluates the r.h.s. of eq. (2.5). This computation has been done in ref. [28] for a 'Goldstone' configuration with

$$\Sigma_{ab} = \delta_{a1} \delta_{b2} - \delta_{a2} \delta_{b1} \quad (6.20)$$

and $\varphi_a \delta_{ab} = \varphi \delta_{ab}$ corresponding to a symmetry breaking pattern with residual $U(2)$ symmetry. The result of ref. [28] can be easily generalized to arbitrary fixed field values of $\tilde{\rho}$ and we find

$$\eta(k) = 4 \frac{v_d}{d} \tilde{\rho} \left[4(\lambda_1)^2 m_{2,2}^d(\epsilon, \epsilon + 2\tilde{\rho}\lambda_1; \eta) + (\lambda_2)^2 m_{2,2}^d(\epsilon, \epsilon + \tilde{\rho}\lambda_2; \eta) \right]. \quad (6.21)$$

The explicit form of the 'threshold' function

$$m_{2,2}^d(\omega_1, \omega_2; \eta) = m_{2,2}^d(\omega_1, \omega_2) - \eta \hat{m}_{2,2}^d(\omega_1, \omega_2) \quad (6.22)$$

can be found in refs. [27, 28]. For vanishing arguments the functions $m_{2,2}^d$ and $\hat{m}_{2,2}^d$ are of order unity. They are symmetric with respect to their arguments and in leading order $m_{2,2}^d(0, \omega) \sim \hat{m}_{2,2}^d(0, \omega) \sim \omega^{-2}$ for $\omega \gg 1$. According to eq. (3.4) we use $\tilde{\rho} = \kappa$ to define the uniform wave function renormalization

$$Z_k \equiv Z_k(\kappa). \quad (6.23)$$

We point out that according to our truncation of the effective average action with eq. (6.21) the anomalous dimension η is exactly zero at $\tilde{\rho} = 0$. This is an artefact of the truncation and we expect the symmetric phase to be more affected by truncation errors than the spontaneously broken phase. We typically observe small values for $\eta(k) = -d(\ln Z_k)/dt$ (of the order of a few per cent). The smallness of η is crucial for our approximation of a uniform wave function renormalization to give quantitatively reliable results for the equation of state. For the universal equation of state given in sect. 8 one has $\eta = 0.022$ as given by the corresponding index of the $O(8)$ symmetric 'vector' model.

7 Renormalization group flow

To understand the detailed picture of the phase structure presented in section 4 we will consider the flow of some characteristic quantities for the effective average potential as the infrared cutoff k is lowered. We will always consider in this section the trajectories for the critical 'temperature', i.e. $\delta\kappa_\Lambda = 0$, and we follow the flow for different values of the short distance parameters $\lambda_{1\Lambda}$ and $\lambda_{2\Lambda}$. The discussion for sufficiently small $\delta\kappa_\Lambda$ is analogous. In particular, we compare the renormalization group flow of these quantities for a weak and a strong first order phase transition. In some limiting cases their behavior can be studied analytically. For the discussion we will frequently consider the flow equations for the quartic 'couplings' $\lambda_1(\tilde{\rho})$, $\lambda_2(\tilde{\rho})$ eqs. (6.8), (6.9) and for the minimum κ eq. (6.15).

In fig. 6, 7 we follow the flow of the dimensionless renormalized minimum κ and the radial mass term $\tilde{m}^2 = 2\kappa\lambda_1(\kappa)$ in comparison to their dimensionful counterparts $\rho_{0R} = k\kappa$ and $m_R^2 = k^2\tilde{m}^2$ in units of the momentum scale Λ . We also consider the dimensionless renormalized mass term $\tilde{m}_2^2 = \kappa\lambda_2(\kappa)$ corresponding to the curvature of the potential in the direction of the second invariant $\tilde{\tau}$. The height of the potential barrier $U_B(k) = k^3 u_k(\tilde{\rho}_B)$ with $u'_k(\tilde{\rho}_B) = 0$, $0 < \tilde{\rho}_B < \kappa$, and the height of the outer minimum $U_0(k) = k^3 u_k(\kappa)$ is also displayed and will be discussed in section 9. Fig. 6 shows these

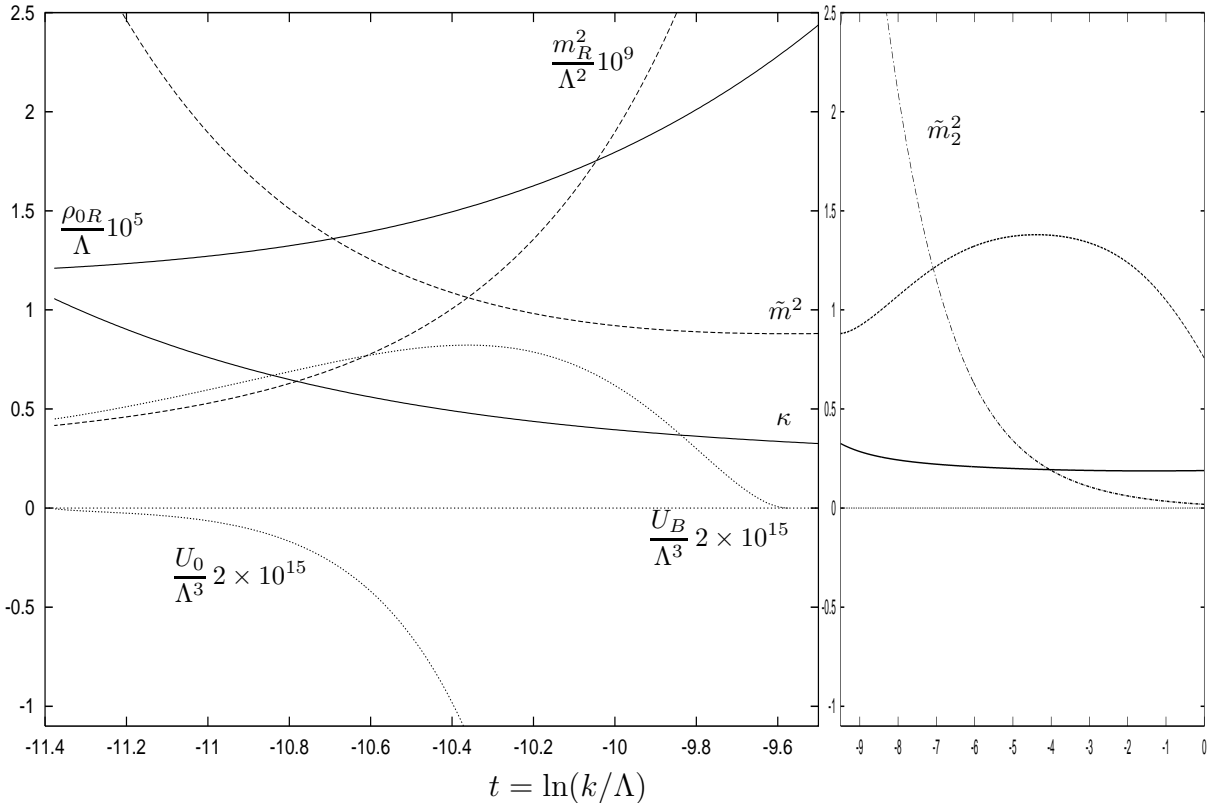


Figure 6: Scale dependence of the dimensionless renormalized masses \tilde{m}^2 , \tilde{m}_2^2 , minimum κ and dimensional counterparts $m_R^2 = k^2 \tilde{m}^2$, $\rho_{0R} = k\kappa$ in units of Λ . We also show $U_B(k)$ and $U_0(k)$, the value of the potential at the top of the potential barrier and at the minimum ρ_{0R} , respectively. The short distance parameters are $\lambda_{1\Lambda} = 2$, $\lambda_{2\Lambda} = 0.1$ and $\delta\kappa_\Lambda = 0$.

quantities as a function of $t = \ln(k/\Lambda)$ for $\lambda_{1\Lambda} = 2$, $\lambda_{2\Lambda} = 0.1$. One observes that the flow can be separated into two parts. The first part ranging from $t = 0$ to $t \simeq -6$ is characterized by $\kappa \simeq \text{const}$ and small \tilde{m}_2^2 . It is instructive to consider what happens in the case $\tilde{m}_2^2 \equiv 0$. In this case $\lambda_2 \equiv 0$ and the flow is governed by the Wilson-Fisher fixed point of the $O(8)$ symmetric theory. At the corresponding second order phase transition the evolution of u_k leads to the scaling solution of (5.15) which obtains for $\partial u_k / \partial t = 0$. As a consequence u_k becomes a k -independent function that takes on constant (fixed point) values [27, 22]. In particular, the minimum κ of the potential takes on its fixed point value $\kappa(k) = \kappa_*$. The fixed point is not attractive in the $U(2) \times U(2)$ symmetric theory and $\lambda_{2\Lambda}$ is an additional relevant parameter for the system. For small λ_2 the evolution is governed by an anomalous dimension $d\lambda_2/dt = A\lambda_2$ with $A < 0$, leading to the increasing \tilde{m}_2^2 as k is lowered.

The system exhibits scaling behavior only for sufficiently small λ_2 . As \tilde{m}_2^2 increases the quartic coupling λ_1 and therefore the radial mass term \tilde{m}^2 is driven to smaller values as can be observed from fig. 6. For nonvanishing λ_2 the corresponding qualitative change in the flow equation (6.8) for λ_1 is the occurrence of a term $\sim \lambda_2^2$. It allows to drive λ_1

to negative values in a certain range of $\tilde{\rho} < \kappa$ and, therefore, to create a potential barrier inducing a first order phase transition. We observe from the plot that at $t \lesssim -9.5$ a second minimum arises ($U_B \neq 0$). The corresponding value of $k = \Lambda e^t = k_2$ sets a characteristic scale for the first order phase transition. Below this scale the dimensionless, renormalized quantities approximately scale according to their canonical dimension. The dimensionful quantities like ρ_{0R} or m_R^2 show only a weak scale dependence in this range. In contrast to the above example of a weak first order phase transition with characteristic renormalized masses much smaller than Λ fig. 7 shows the flow of the corresponding quantities for a strong first order phase transition. The short distance parameters employed are $\lambda_{1\Lambda} = 0.1$, $\lambda_{2\Lambda} = 2$. Here the range with $\kappa \simeq \text{const}$ is almost absent and one observes no approximate scaling behavior.

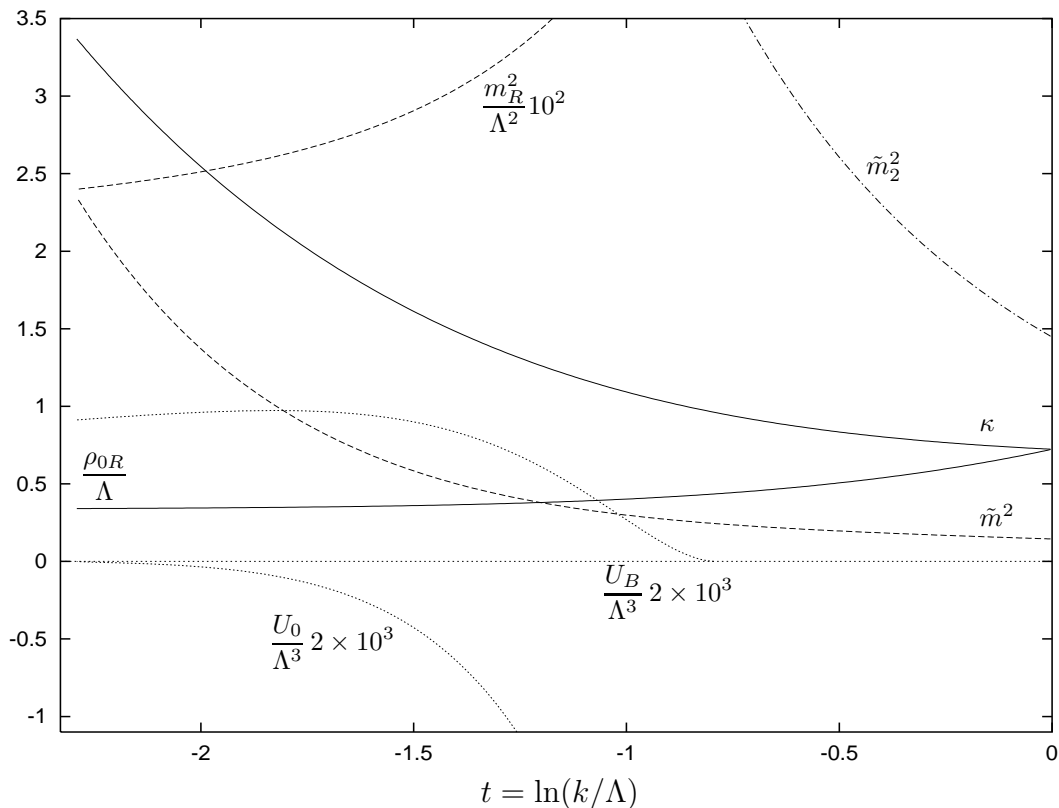


Figure 7: Same as fig. 6 for $\lambda_{1\Lambda} = 0.1$ and $\lambda_{2\Lambda} = 2$.

With the above examples it becomes easy to understand the phase structure presented in section 4. For the given curves of figs. 4 and 5 we distinguished between the range $\lambda_{2\Lambda}/\lambda_{1\Lambda} \ll 1$ and $\lambda_{2\Lambda}/\lambda_{1\Lambda} \gg 1$ to denote the weak and the strong first order region. For $\lambda_{2\Lambda}/\lambda_{1\Lambda} \ll 1$ the initial renormalization group flow is dominated by the Wilson-Fisher fixed point of the $O(8)$ symmetric theory. In this range the irrelevant couplings are driven close to the fixed point for some 'time' $|t| = -\ln(k/\Lambda)$, losing their memory on the initial conditions given by the short distance potential u_Λ . As a consequence we are able

to observe universal behavior as is demonstrated in fig. 5.

To discuss the case $\lambda_{2\Lambda}/\lambda_{1\Lambda} \gg 1$ we consider the flow equations for the couplings at the minimum $\kappa \neq 0$ of the potential given by (6.15) and (6.16) with (6.8), (6.9). In the limit of an infinite mass term $\tilde{m}_2^2 = \kappa\lambda_2(\kappa) \rightarrow \infty$ the β -functions for $\lambda_1(\kappa)$ and κ become independent from $\lambda_2(\kappa)$ due to the 'threshold' functions, with $l_n^3(\kappa\lambda_2) \sim (\kappa\lambda_2)^{-(n+1)}$ for large $\kappa\lambda_2(\kappa)$. As a consequence β_{λ_1} and β_κ equal the β -functions for an $O(5)$ symmetric model. We argue in the following that in this large coupling limit fluctuations of massless Goldstone bosons lead to an attractive fixed point for $\lambda_2(\kappa)$. We take the flow equation (6.16), (6.9) for $\lambda_2(\kappa)$ keeping only terms with positive canonical mass dimension for a qualitative discussion. (This amounts to the approximation $\lambda_1^{(n)}(\kappa) = \lambda_2^{(n)}(\kappa) = 0$ for $n \geq 1$.) To be explicit, one may consider the case for given $\lambda_{1\Lambda} = 2$. The critical cutoff value for the potential minimum is $\kappa_\Lambda \simeq 0.2$ for $\lambda_{2\Lambda} \gg 1$. For $\kappa\lambda_2(\kappa) \gg 1$ and taking $\eta \simeq 0$ the β -function for $\lambda_2(\kappa)$ is to a good approximation given by ($d = 3$)

$$\frac{d\lambda_2(\kappa)}{dt} = -\lambda_2(\kappa) + 2v_3(\lambda_2(\kappa))^2 l_2^3(0). \quad (7.1)$$

The second term on the r.h.s. of eq. (7.1) is due to massless Goldstone modes which give the dominant contribution in the considered range. The solution of (7.1) implies an attractive fixed point for $\lambda_2(\kappa)$ with a value

$$\lambda_{2\star}(\kappa) = \frac{1}{2v_3 l_2^3(0)} \simeq 4\pi^2. \quad (7.2)$$

Starting from $\lambda_{2\Lambda}$ one finds for the 'time' $|t|$ necessary to reach a given $\lambda_2(\kappa) > \lambda_{2\star}(\kappa)$

$$|t| = -\ln \frac{\lambda_2(\kappa) - \lambda_{2\star}(\kappa)}{\lambda_2(\kappa) \left(1 - \frac{\lambda_{2\star}(\kappa)}{\lambda_{2\Lambda}}\right)}. \quad (7.3)$$

This converges to a finite value for $\lambda_{2\Lambda} \rightarrow \infty$. The further evolution therefore becomes insensitive to the initial value for $\lambda_{2\Lambda}$ in the large coupling limit. The flow of $\lambda_1(\kappa)$ and κ is not affected by the initial running of $\lambda_2(\kappa)$ and quantities like $\Delta\rho_{0R}/\Lambda$ or $m_R/\Delta\rho_{0R}$ become independent of $\lambda_{2\Lambda}$ if the coupling is sufficiently large. This qualitative discussion is confirmed by the numerical solution of the full set of equations presented in figs. 4 and 5. For the fixed point value we obtain $\lambda_{2\star}(\kappa) = 38.02$. We point out that an analogous discussion for the large coupling region of $\lambda_{1\Lambda}$ cannot be made. This can be seen by considering the mass term at the origin of the short distance potential (3.6) given by $u'_\Lambda(0,0) = -\kappa_\Lambda \lambda_{1\Lambda}$. Due to the pole of $l_n^3(\omega, \eta)$ at $\omega = -1$ for $n > 1/2$ (cf. appendix A) one obtains the constraint

$$\kappa_\Lambda \lambda_{1\Lambda} < 1 \quad . \quad (7.4)$$

In the limit $\lambda_{1\Lambda} \rightarrow \infty$ the mass term $2\kappa_\Lambda \lambda_{1\Lambda}$ at the minimum κ of the potential at the critical temperature therefore remains finite.

8 Scaling equation of state for weak first order phase transitions

We presented in section 4 some characteristic quantities for the effective average potential which become universal at the phase transition for a sufficiently small quartic coupling $\lambda_{2\Lambda} = \bar{\lambda}_{2\Lambda}/\Lambda$ of the short distance potential U_Λ (3.6). The aim of this section is to generalize this observation and to find a universal scaling form of the equation of state for weak first order phase transitions. The equation of state relates the derivative of the free energy $U = \lim_{k \rightarrow 0} U_k$ to an external source, $\partial U / \partial \varphi = j$. Here the derivative has to be evaluated in the outer convex region of the potential. For instance, for the meson model of strong interactions the source j is proportional to the average quark mass [8, 36] and the equation of state permits to study the quark mass dependence of properties of the chiral phase transition. We will compute the equation of state for a nonzero coarse graining scale k . It therefore contains information for quantities like the 'classical' bubble surface tension in the context of Langer's theory of bubble formation which will be discussed in section 9.

In three dimensions the $U(2) \times U(2)$ symmetric model exhibits a second order phase transition in the limit of a vanishing quartic coupling $\lambda_{2\Lambda}$ due to an enhanced $O(8)$ symmetry. In this case there is no scale present in the theory at the critical temperature. In the vicinity of the critical temperature (small $|\delta\kappa_\Lambda| \sim |T_c - T|$) and for small enough $\lambda_{2\Lambda}$ one therefore expects a scaling behavior of the effective average potential U_k and accordingly a universal scaling form of the equation of state. At the second order phase transition in the $O(8)$ symmetric model there are only two independent scales that can be related to the deviation from the critical temperature and to the external source or φ . As a consequence the properly rescaled potential U/ρ_R^3 or $U/\rho^{(\delta+1)/2}$ (with the usual critical exponent δ) can only depend on one dimensionless ratio. A possible set of variables to represent the two independent scales are the renormalized minimum of the potential $\varphi_{0R} = (\rho_{0R}/2)^{1/2}$ (or the renormalized mass for the symmetric phase) and the renormalized field $\varphi_R = (\rho_R/2)^{1/2}$. The rescaled potential will then only depend on the scaling variable $z = \varphi_R/\varphi_{0R}$ [15]. Another possible choice is the Widom scaling variable $x = -\delta\kappa_\Lambda/\varphi^{1/\beta}$ [38]. In the $U(2) \times U(2)$ symmetric theory $\lambda_{2\Lambda}$ is an additional relevant parameter which renders the phase transition first order and introduces a new scale, e.g. the nonvanishing value for the jump in the renormalized order parameter $\Delta\varphi_{0R} = (\Delta\rho_{0R}/2)^{1/2}$ at the critical temperature or $\delta\kappa_\Lambda = 0$. In the universal range we therefore observe three independent scales and the scaling form of the equation of state will depend on two dimensionless ratios. The rescaled potential U/φ_{0R}^6 can then be written as a universal function G

$$\frac{U}{\varphi_{0R}^6} = G(z, v) \quad (8.1)$$

which depends on the two scaling variables

$$z = \frac{\varphi_R}{\varphi_{0R}}, \quad v = \frac{\Delta\varphi_{0R}}{\varphi_{0R}}. \quad (8.2)$$

The relation (8.1) is the scaling form of the equation of state we are looking for. At a second order phase transition the variable v vanishes identically and $G(z, 0)$ describes the scaling equation of state for the model with $O(8)$ symmetry [15]. The variable v accounts for the additional scale present at the first order phase transition. We note that $z = 1$ corresponds to a vanishing source and $G(1, v)$ describes the temperature dependence of the free energy for $j = 0$. In this case $v = 1$ denotes the critical temperature T_c whereas for $T < T_c$ one has $v < 1$. Accordingly $v > 1$ obtains for $T > T_c$ and φ_{0R} describes here the local minimum corresponding to the metastable ordered phase. The function $G(z, 1)$ accounts for the dependence of the free energy on j for $T = T_c$.

We consider the scaling form (8.1) of the equation of state for a nonzero coarse graining scale k . The renormalized field is given by $\varphi_R = Z_k^{1/2} \varphi$. We pointed out in section 4 that there is a characteristic scale k_2 for the first order phase transition where the second local minimum of the effective average potential appears. For weak first order phase transitions one finds $\rho_{0R} \sim k_2$. To observe the scaling form of the equation of state the infrared cutoff k has to run below k_2 with $k \ll k_2$. For the scale k_f defined in eq. (4.11) we observe universal behavior to high accuracy (cf. fig. 5 and the corresponding universal ratios in table 1 for small $\lambda_{2\Lambda}/\lambda_{1\Lambda}$). The result for the universal function $U_{k_f}/\varphi_{0R}^6 = G_{k_f}(z, v)$ is presented in fig. 8. For $v = 1$ one has $\varphi_{0R}(k_f) = \Delta\varphi_{0R}(k_f)$ which denotes the critical temperature. Accordingly $v > 1$ denotes temperatures above and $v < 1$ temperatures below the critical temperature. One observes that $G_{k_f}(z, 1)$ shows two almost degenerate minima. (They become exactly degenerate in the limit $k \rightarrow 0$). For the given examples $v = 1.18, 1.07$ the minimum at the origin becomes the absolute minimum and the system is in the symmetric phase. In contrast, for $v = 0.90, 0.74$ the absolute minimum is located at $z = 1$ which characterizes the spontaneously broken phase. For small enough v the local minimum at the origin vanishes.

We explicitly verified that the universal function G_{k_f} depends only on the scaling variables z and v by choosing various values for $\delta\kappa_\Lambda$ and for the quartic couplings of the short distance potential, $\lambda_{1\Lambda}$ and $\lambda_{2\Lambda}$. In section 4 we observed that the model shows universal behavior for a certain range of the parameter space. For given $\lambda_{1\Lambda}$ and small enough $\lambda_{2\Lambda}$ one always observes universal behavior. For $\lambda_{1\Lambda} = 0.1, 2$ and 4 it is demonstrated that (approximate) universality holds for $\lambda_{2\Lambda}/\lambda_{1\Lambda} \lesssim 1/2$ (cf. fig. 5). For $\lambda_{1\Lambda}$ around 2 one observes from figs. 4, 5 and table 1 that the system is to a good accuracy described by its universal properties for even larger values of $\lambda_{2\Lambda}$. The corresponding phase transitions cannot be considered as particularly weak first order. The universal function G_{k_f} therefore accounts for a quite large range of the parameter space.

We emphasize that the universal form of the effective potential given in fig. 8 depends on the scale k_f where the integration of the flow equations is stopped (cf. eq. (4.11)). A different prescription for k_f will, in general, lead to a different form of the effective potential. We may interpret this as a scheme dependence describing the effect of different coarse graining procedures. This is fundamentally different from nonuniversal corrections since G_{k_f} is completely independent of details of the short distance or classical action and in this sense universal. A more quantitative discussion of this scheme dependence will be presented in the next section. We note that fluctuations on scales $k < k_f$ do not

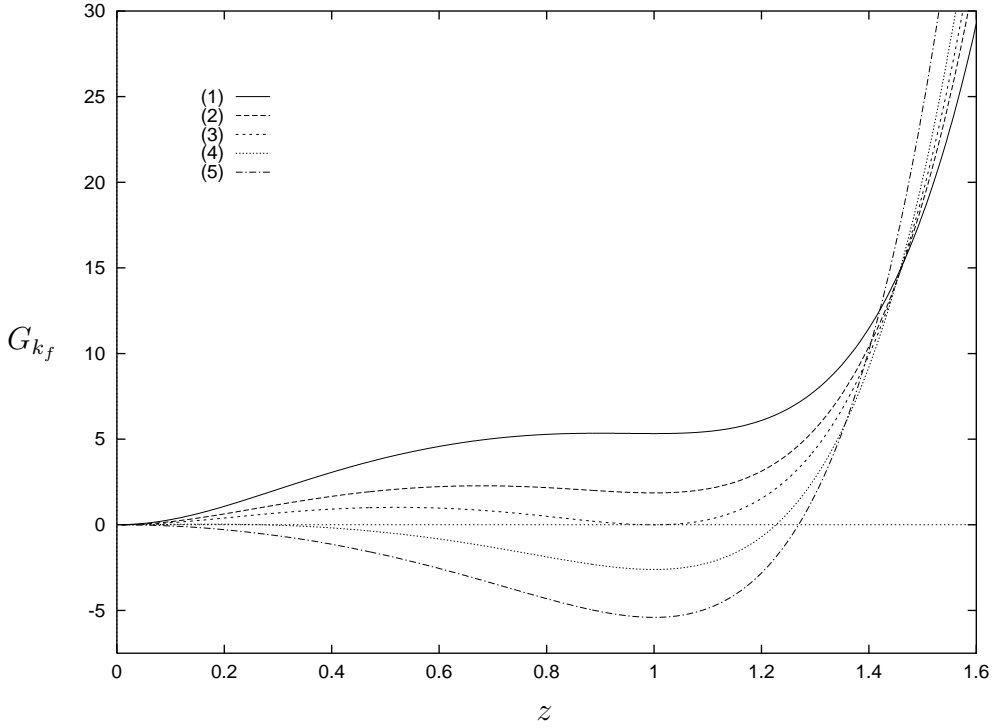


Figure 8: Universal shape of the coarse grained potential ($k = k_f$) as a function of the scaling variable $z = \varphi_R/\varphi_{0R} = (\rho_R/\rho_{0R})^{1/2}$ for different values of $v = \Delta\varphi_{0R}/\varphi_{0R} = (\Delta\rho_{0R}/\rho_{0R})^{1/2}$. The employed values for v are (1) $v = 1.18$, (2) $v = 1.07$, (3) $v = 1$, (4) $v = 0.90$, (5) $v = 0.74$. For vanishing sources one has $z = 1$. In this case $v = 1$ denotes the critical temperature T_c . Similarly $v > 1$ corresponds to $T > T_c$ with φ_{0R} denoting the minimum in the metastable ordered phase.

influence substantially the location of the minima of the coarse grained potential and the form of $U_k(\varphi_R)$ for $\varphi_R > \varphi_{0R}$ remains almost k -independent. Here $\partial U_{k_f}/\partial\varphi = j(k_f)$ with $j(k_f) \simeq \lim_{k \rightarrow 0} j(k) = j$.⁶

We have established the scaling equation of state using the renormalized variables φ_R , φ_{0R} and $\Delta\varphi_{0R}$. Alternatively the scaling equation of state can be presented in terms of the short distance parameters $\delta\kappa_\Lambda$, $\lambda_{2\Lambda}$ and the unrenormalized field φ . For the $O(8)$ symmetric model ($\lambda_{2\Lambda} = 0$) this is known as the Widom scaling form of the equation of state [38] and in this case the relation between φ_R , φ_{0R} and φ , $\delta\kappa_\Lambda$ is solely determined by critical exponents and amplitudes [15]. For the $U(2) \times U(2)$ symmetric model the dependence of φ_R , φ_{0R} and $\Delta\varphi_{0R}$ on the parameters $\delta\kappa_\Lambda$, $\lambda_{2\Lambda}$ and the unrenormalized field φ can be expressed in terms of scaling functions. In general, only for limiting cases as $\delta\kappa_\Lambda = 0$ or $\lambda_{2\Lambda} = 0$ the relation is determined by critical exponents and amplitudes. We will consider here these limits. The computation of the scaling functions for the general case as well as the corresponding (generalized) Widom scaling form of the equation of state is the subject of a separate work [39].

⁶The role of massless Goldstone boson fluctuations for the universal form of the effective average potential in the limit $k \rightarrow 0$ has been discussed previously for the $O(8)$ symmetric model [15].

We consider the renormalized minimum φ_{0R} in two limits which are denoted by $\Delta\varphi_{0R} = \varphi_{0R}(\delta\kappa_\Lambda = 0)$ and $\varphi_{0R}^0 = \varphi_{0R}(\lambda_{2\Lambda} = 0)$. The behavior of $\Delta\varphi_{0R}$ is described in terms of the exponent θ according to eq. (4.7),

$$\Delta\varphi_{0R} \sim (\lambda_{2\Lambda})^{\theta/2}, \quad \theta = 1.93. \quad (8.3)$$

The dependence of the minimum φ_{0R}^0 of the $O(8)$ symmetric potential on the temperature is characterized by the critical exponent ν ,

$$\varphi_{0R}^0 \sim (\delta\kappa_\Lambda)^{\nu/2}, \quad \nu = 0.882. \quad (8.4)$$

The exponent ν for the $O(8)$ symmetric model is determined analogously to θ as described in section 4⁷. We can also introduce a critical exponent ζ for the jump of the unrenormalized order parameter

$$\Delta\varphi_0 \sim (\lambda_{2\Lambda})^\zeta, \quad \zeta = 0.988. \quad (8.5)$$

With

$$\varphi_0^0 \sim (\delta\kappa_\Lambda)^\beta, \quad \beta = 0.451 \quad (8.6)$$

it is related to θ and ν by the additional index relation

$$\frac{\theta}{\zeta} = \frac{\nu}{\beta} = 1.95. \quad (8.7)$$

We have verified this numerically. For the case $\delta\kappa_\Lambda = \lambda_{2\Lambda} = 0$ one obtains

$$j \sim \varphi^\delta. \quad (8.8)$$

The exponent δ is related to the anomalous dimension η via the usual index relation $\delta = (5 - \eta)/(1 + \eta)$. From the scaling solution of eq. (6.21) we obtain $\eta = 0.0224$.

With the help of the above relations one immediately verifies that for $\lambda_{2\Lambda} = 0$

$$z \sim (-x)^{-\beta}, \quad v = 0 \quad (8.9)$$

and for $\delta\kappa_\Lambda = 0$

$$z \sim y^{-\zeta}, \quad v = 1. \quad (8.10)$$

Here we have used the Widom scaling variable x and the new scaling variable y given by

$$x = \frac{-x}{\varphi^{1/\beta}}, \quad y = \frac{\lambda_{2\Lambda}}{\varphi^{1/\zeta}}. \quad (8.11)$$

⁷For the $O(8)$ symmetric model ($\lambda_{2\Lambda} = 0$) we consider the minimum φ_{0R}^0 at $k = 0$.

9 Coarse graining and Langer's theory of bubble formation

The coarse grained effective potential U_k results from the integration of fluctuations with momenta larger than $\sim k$. It is a nonconvex function whereas the standard effective potential $U = \lim_{k \rightarrow 0} U_k$ has to be convex by its definition as a Legendre transform. The difference between U and U_k is due to fluctuations with characteristic length scales larger than the inverse coarse graining scale $\sim k^{-1}$. The role of these fluctuations for the approach to convexity has been established explicitly [26]. The study of first order phase transitions usually relies on the nonconvex 'part' of the potential. As an illustration we consider the change of the system from the high temperature to the low temperature phase by bubble nucleation as described by Langer's theory [17]. On the one hand, the approach relies on the definition of a suitable coarse grained free energy Γ_k with a coarse graining scale k and, on the other hand, a saddle point approximation for the treatment of fluctuations around the 'critical bubble' is employed. The problem is therefore separated into two parts: One part concerns the treatment of fluctuations with momenta $q^2 \gtrsim k^2$ which are included in the coarse grained free energy. The second part deals with an estimate of fluctuations around the bubble for which only fluctuations with momenta smaller than k must be considered. These issues will be discussed in this section in a quantitative way. In particular, we will give a criterion for the validity of Langer's formula.

One may consider a system that starts at some high temperature $T > T_c$ and investigate what happens as T is lowered as a function of time as for example during the evolution of the early universe. For large enough temperature the origin of the potential ($\varphi = 0$) is the only minimum and the system is therefore originally in the symmetric phase. As T approaches T_c a second local minimum develops at $\varphi_0 > 0$. This becomes the absolute minimum below T_c . Nevertheless, the potential barrier prevents the system to change smoothly to the ordered phase. For a short while where T is in the vicinity of T_c but below T_c the system remains therefore in a state with higher energy density as compared to the state corresponding to the absolute minimum away from the origin. This is the so-called 'false vacuum' in high energy physics or the metastable state in statistical physics. Such a state is unstable with respect to fluctuations which penetrate or cross the barrier. The picture is familiar from the condensation of vapor. The false vacuum corresponds to the supercooled vapor phase and the true vacuum to the fluid phase. Bubbles of the true vacuum (droplets) occur through thermal or quantum fluctuations⁸. If a bubble is large enough so that the decrease in volume energy exceeds the surface energy it will grow. The phase transition is completed once the whole space is filled with the true vacuum. On the other hand, small bubbles shrink due to the surface tension. The critical bubble is just large enough that it does not shrink. To be explicit we consider a spherical bubble where the bubble wall with 'thickness' Δ is thin as compared to the bubble radius R , i.e. $\Delta \ll R$. In leading order the coarse grained free energy Γ_k for such

⁸In the real world the condensation of vapor is triggered by impurities but this is not the issue here.

a bubble configuration can be decomposed in a volume and a surface term [40, 41]

$$\Gamma_k^{(0)} = -\frac{4\pi}{3}R^3\epsilon + 4\pi R^2\sigma_k. \quad (9.1)$$

In the thin wall approximation one obtains for the surface tension σ_k in our conventions

$$\sigma_k = 2 \int_0^{\varphi_0} d\varphi \sqrt{2Z_k U_k(\varphi)}. \quad (9.2)$$

For the difference in the free energy density ϵ one has

$$\epsilon = U(0) - U(\varphi_0) = -\lim_{k \rightarrow 0} U_0(k). \quad (9.3)$$

We include in ϵ fluctuations with arbitrarily small momenta. In contrast, the long wavelength contributions to σ_k are effectively cut off by the characteristic length scale of the bubble surface and are described by the 'fluctuation determinant' A_k (cf. eq. (9.4)). The determination of a suitable coarse graining scale k for the computation of σ_k is discussed below.

The critical bubble maximizes $\Gamma_k^{(0)}$ with respect to the radius. It minimizes the coarse grained free energy with respect to other deformations because the spherical form is energetically favorable. The critical bubble therefore represents a saddle point in the space of possible 'bubble configurations'. In Langer's theory of bubble formation one considers a saddle point expansion around the critical bubble. There is exactly one negative mode that corresponds to the shrinking or growth of the bubble and there are infinitely many positive modes (there are also translational zero modes)⁹. The bubble nucleation rate $\bar{\Gamma}$, which describes the probability per unit volume per unit time for the transition to the new vacuum, can be written in the form [40, 41]

$$\bar{\Gamma} = A_k \exp(-\Gamma_k^{(0)}[\varphi_b^{(0)}]) = A_k \exp\left(-\frac{16\pi}{3} \frac{\sigma_k^3}{\epsilon^2}\right) \quad (9.4)$$

where $\Gamma_k^{(0)}$ is evaluated for $\varphi_b^{(0)}$ corresponding to the critical bubble and approximated by (9.1). The exponential term with the coarse grained free energy $\Gamma_k^{(0)}$ denotes the lowest order or classical contribution. The prefactor A_k contains several factors that depend on the details of the system under investigation. In particular, A_k accounts for the contribution to the free energy from the fluctuations with momenta smaller than k . It depends on k through the effective ultraviolet cutoff for these fluctuations which is present since fluctuations with momenta larger than k are already included in $\Gamma_k^{(0)}[\varphi_b^{(0)}]$ ¹⁰.

⁹Langer's theory is not restricted to the thin wall approximation which is considered here for simplicity. In particular, the property of the critical bubble to represent a saddle point with exactly one negative mode is independent from the thin wall approximation.

¹⁰The effective average action [18] also provides the formal tool how the ultraviolet cutoff $\sim k$ is implemented in the remaining functional integral for large length scale fluctuations.

Langer's formula for bubble nucleation amounts essentially to a perturbative one loop estimate of A_k .

For a determination of a useful choice of k it is convenient to place the discussion in a more general context which does not rely on the thin wall approximation or a saddle point approximation. What one is finally interested in is the free energy $\Gamma[\varphi_b]$ for bubble configurations of a given shape. The 'true critical bubble' φ_b^c corresponds to a saddle point in the space of 'bubble configurations' which are characterized by boundary conditions connecting the false and the true vacuum. The nucleation rate is then proportional $\exp -\Gamma[\varphi_b^c]$. The coarse graining can be seen as a convenient strategy to evaluate $\Gamma[\varphi_b]$ by separating contributions from different momentum scales. We propose to choose the coarse graining scale k somewhat above but in the vicinity of the inverse thickness Δ^{-1} of the bubble wall. We will argue below that in this case the corrections to the effective surface tension from the prefactor A_k should be best accessible.

In fact, we can write $\bar{\Gamma} = B \exp -\Gamma[\varphi_b^c]$ where B contains dynamical factors and $\Gamma[\varphi_b^c]$ does not include contributions from fluctuations of the negative mode and the translational modes present for the critical bubble. The prefactor in eq. (9.4) can then be written as

$$A_k = B \exp -(\delta_k + \eta_k) \tag{9.5}$$

where

$$\delta_k = \Gamma[\varphi_b^c] - \Gamma_k[\varphi_b^c], \quad \eta_k = \Gamma_k[\varphi_b^c] - \frac{16\pi}{3} \frac{\sigma_k^3}{\epsilon^2}. \tag{9.6}$$

The term η_k includes the difference between the true critical bubble and the configuration used to estimate σ_k as well as a correction term to ϵ to be discussed below. We first concentrate on δ_k which describes the difference between the free energy and the coarse grained free energy for the critical bubble. As mentioned above this is due to fluctuations with momenta $q^2 \lesssim k^2$ and incorporates the dominant k -dependence of A_k . Since the bubble provides for inherent effective infrared cutoff scales $\sim R^{-1}$ or Δ^{-1} the contribution δ_k is both infrared and ultraviolet finite. The larger k , the more fluctuations are included in δ_k and from this point of view one wants to take k as low as possible. On the other hand, k should not be taken smaller than Δ^{-1} if the approximation used for a computation of Γ_k relies on almost constant field configurations rather than real bubbles, as is usually the case. Only for k sufficiently large compared to Δ^{-1} the difference between an evaluation of the potential and kinetic terms in Γ_k for almost constant field configurations (e.g. by a derivative expansion) rather than for bubbles remains small. In this way the technique of course graining combines a relatively simple treatment of the modes with $q^2 \gtrsim k^2$ for which the detailed properties of the bubble are irrelevant with an estimate of fluctuations around the bubble for which the short distance physics ($q^2 \gtrsim k^2$) needs not to be considered anymore. It is clear that k is only a technical construct and for physical quantities the k -dependence of δ_k and $\Gamma_k^{(0)}$ must cancel. More precisely, this concerns the sum $\delta_k + \eta_k + 16\pi\sigma_k^3/3\epsilon^2$. For thin wall bubbles the most important contribution to η_k is easily identified: By our definition of ϵ we have included contributions from fluctuations with length scales $\gtrsim R$. They should not be present in the effective action for a bubble with finite radius. Therefore η_k contains a correction term $(16\pi/3)\sigma_k^3(\epsilon^{-2}(R) - \epsilon^{-2})$ which

replaces effectively ϵ by $\epsilon(R)$ in eq. (9.4). We can evaluate $\epsilon(R)$ in terms of the coarse grained free energy at a scale k_R

$$\epsilon(R) \simeq U_{k_R}(0) - U_{k_R}(\varphi_0) = -U_0(k_R), \quad k_R = \frac{1}{R}. \quad (9.7)$$

For $\Delta \ll R$ one should not confound k_R with the coarse graining scale k since one has the inequality

$$k_R \ll \frac{1}{\Delta} \lesssim k. \quad (9.8)$$

Only for $\Delta \simeq R$ the clear separation between k_R and k disappears. We note that at the critical temperature one has $R \rightarrow \infty$ and therefore $\epsilon(R) = \epsilon$.

Since σ_k enters the nucleation rate (9.4) exponentially even small changes with k will have large effects. If one finds a strong dependence of σ_k on the coarse graining scale k this is only compatible with a large contribution from the higher orders of the saddle point expansion. The k -dependence of σ_k therefore gives direct information about the validity of Langer's formula. We find a strong scale dependence of σ_k if the phase transition is characterized by large effective dimensionless couplings $\frac{\lambda_R}{m_R^2}(k)$. A weak scale dependence is observed for small effective couplings. This gives a very consistent picture: The validity of the saddle point approximation typically requires small dimensionless couplings. In this case also the details of the coarse graining are not of crucial importance within an appropriate range of k . The remaining part of this section provides a detailed quantitative discussion.

We consider the dependence of the effective average potential U_k and the surface tension σ_k on the coarse graining scale k near the critical temperature T_c for three examples in detail. They are distinguished by different choices for the quartic couplings $\bar{\lambda}_{1\Lambda}$ and $\bar{\lambda}_{2\Lambda}$ of the short distance potential U_Λ given by eq. (3.6). The choice $\bar{\lambda}_{1\Lambda}/\Lambda = 0.1$ and $\bar{\lambda}_{2\Lambda}/\Lambda = 2$ corresponds to a strong first order phase transition with renormalized masses not much smaller than the cutoff scale Λ . The renormalized couplings will turn out small enough such that the notion of a coarse grained potential U_k and a surface tension σ_k can be used without detailed information on the coarse graining scale within a certain range of k . In contrast we give two examples where the dependence of U_k and σ_k on the coarse graining scale becomes of crucial importance. The choice $\bar{\lambda}_{1\Lambda}/\Lambda = 2$ and $\bar{\lambda}_{2\Lambda}/\Lambda = 0.1$ leads to a weak first order phase transition with small renormalized masses and the system shows universal behavior (cf. sect. 4). For $\bar{\lambda}_{1\Lambda}/\Lambda = 4$ and $\bar{\lambda}_{2\Lambda}/\Lambda = 70$ one observes a relatively strong first order phase transition. Nevertheless for both examples the coarse grained potential and the surface tension show a similarly high sensitivity on the scale k .

In figs. 9, 10 the scale dependence of U_k is shown for a fixed temperature in the vicinity of $T = T_c$ or $\delta\kappa_\Lambda = 0$. We plot U_k in units of Λ^3 as a function of $\varphi_R/\Lambda^{1/2} = (\rho_R/2\Lambda)^{1/2} = (Z_k\rho/2\Lambda)^{1/2}$ for different values of k . Each curve differs in $k = \Lambda e^t$ by $\Delta t = 1/18$ and the first curve to the left with a negative curvature at the origin corresponds to $t \simeq -0.40$ for fig. 9 ($t \simeq -9.3$ for fig. 10). For $0 \geq t \gtrsim -0.40$ ($0 \geq t \gtrsim -9.3$) there is only one minimum of the potential away from the origin which lies below the plotted range in fig. 9 (10). Lowering k results in a successive inclusion of fluctuations on larger length

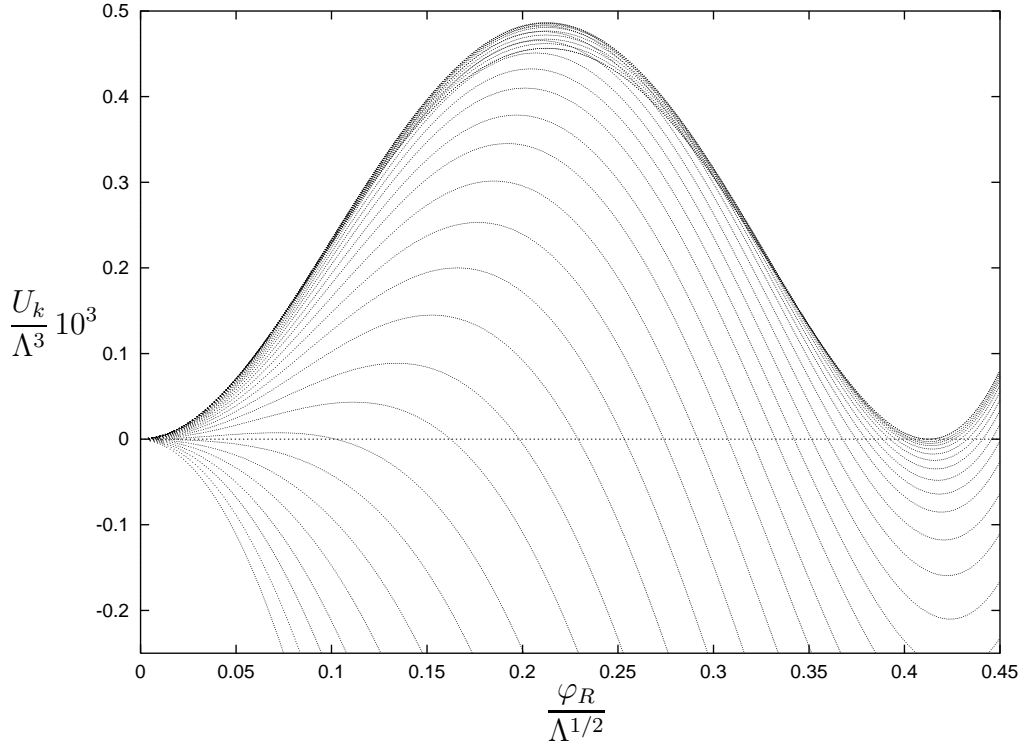


Figure 9: The coarse grained potential in dependence on the coarse graining scale k for fixed (almost critical) temperature. The example corresponds to $\bar{\lambda}_{1\Lambda}/\Lambda = 0.1, \bar{\lambda}_{2\Lambda}/\Lambda = 2$.

scales and one observes the appearance of a second local minimum at the origin of the potential. The barrier between both minima increases and reaches its maximum value. As k is lowered further the potential barrier starts to decrease whereas the location of the minima becomes almost k -independent and degenerate in height. In this region also the outer convex part of the potential shows an almost stable profile due to the decoupling of the massive modes. We stop the integration at the scale $k = k_f$ given by eq. (4.11). The coarse grained effective potential U_k with $k = k_f$ essentially includes all fluctuations with squared momenta larger than the scale $|m_{B,R}^2|$ given by the curvature at the top of the potential barrier (cf. eq. (4.10)). Successive inclusion of fluctuations with momenta smaller than k_f would result in a further decrease of the potential barrier. The flattening of the barrier is induced by the pole structure of the 'threshold' functions $l_n^3(\omega)$ appearing in the flow equations for the couplings (e.g. $l_1^3(\omega)$ appearing in eq. (6.8) exhibits a pole at $\omega = -1$ according to $l_1^3(\omega) \sim (\omega + 1)^{-1/2}$ for ω near -1 (cf. appendix A)). The argument ω corresponds to dimensionless mass terms as $U'_k(\rho_R)/k^2$ or $(U'_k(\rho_R) + 2\rho_R U''_k(\rho_R))/k^2$. In the nonconvex region of the potential the curvature is negative. Since the pole cannot be crossed, negative U'_k or U''_k must go to zero with k^2 and as a consequence the potential barrier flattens. For the scalar 'vector' model the approach to convexity in the limit $k \rightarrow 0$ has been studied analytically previously [26]. Here we are interested in the potential for a nonzero coarse graining scale k .

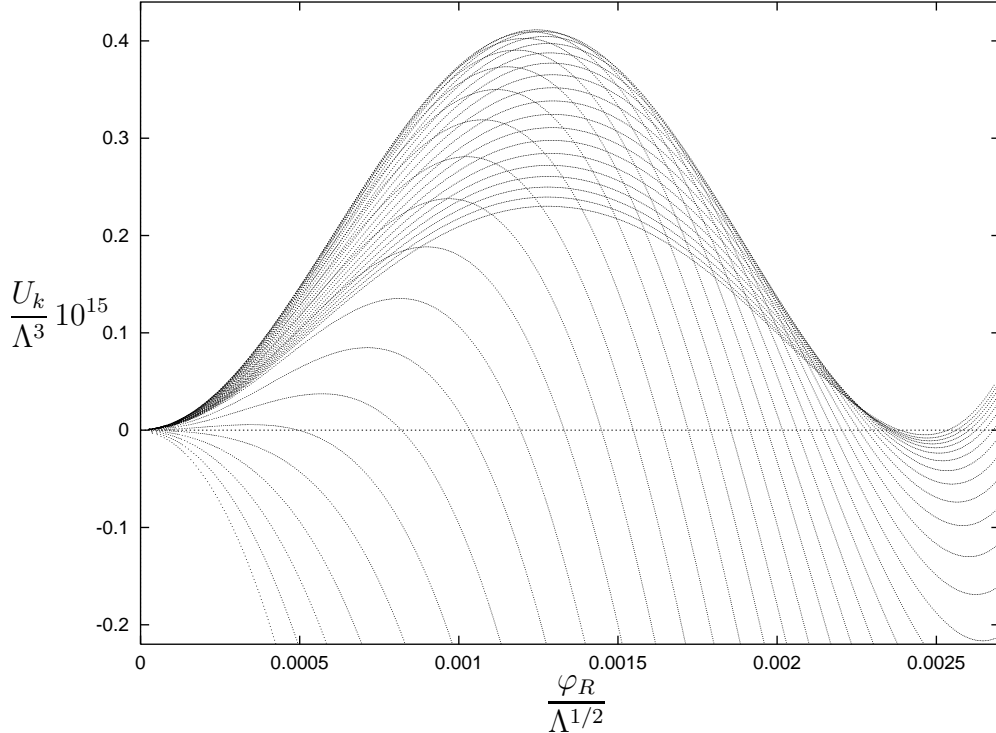


Figure 10: The coarse grained potential for $\bar{\lambda}_{1\Lambda}/\Lambda = 2, \bar{\lambda}_{2\Lambda}/\Lambda = 0.1$.

The most significant difference between fig. 9 and fig. 10 is the k -dependence of the potential barrier in a region where the minima become degenerate and almost independent of k . Fig. 9 shows a barrier with a weak scale dependence in the range of k where the location of the minima stabilizes. In contrast, in fig. 10 one observes a barrier with a strong scale dependence in this region. Figs. 6 and 7 (cf. sect. 7) show the relative height $U_0(k) = U_k(\varphi_0) - U_k(0)$ between the two local minima and the height of the potential barrier $U_B(k) = U_k(\varphi_B) - U_k(0)$ ($(\partial U_k / \partial \varphi)(\varphi_B) = 0, 0 < \varphi_B < \varphi_0$) as a function of $t = \ln(k/\Lambda)$. Accordingly one observes that for $\bar{\lambda}_{1\Lambda}/\Lambda = 0.1, \bar{\lambda}_{2\Lambda}/\Lambda = 2$ the top of the potential barrier shows a weak scale dependence in a region of k where $U_0(k)$ is small whereas for $\bar{\lambda}_{1\Lambda}/\Lambda = 2, \bar{\lambda}_{2\Lambda}/\Lambda = 0.1$ the top of the potential barrier depends strongly on the coarse graining scale in this region. The surface tension σ_k is displayed in fig. 11 and shows a corresponding behavior. Here we consider σ_k also for the short distance parameters $\bar{\lambda}_{1\Lambda}/\Lambda = 4, \bar{\lambda}_{2\Lambda}/\Lambda = 70$. In fig. 11 the surface tension σ_k is normalized to σ_{\max} ($\sigma_{\max}/\Lambda^2 = 1.67 \times 10^{-2}(8.41 \times 10^{-11})(1.01 \times 10^{-3})$ for $\bar{\lambda}_{1\Lambda}/\Lambda = 0.1(2)(4), \bar{\lambda}_{2\Lambda}/\Lambda = 2(0.1)(70)$) and given as a function of $\ln(k/k_f)$.¹¹ For $\bar{\lambda}_{1\Lambda}/\Lambda = 0.1, \bar{\lambda}_{2\Lambda}/\Lambda = 2$ the curve exhibits a small curvature around its maximum and $\sigma_{\max} \simeq \sigma_{k=k_f}$. One observes for the second and the third example a comparably large curvature around σ_{\max} and $\sigma_{k=k_f}$ becomes considerably smaller than the maximum. One may consider what happens if

¹¹The integration according to eq. (9.2) is performed between the two zeros $\varphi = 0$ and $\varphi = \varphi'_0 \lesssim \varphi_0$ of U_k .

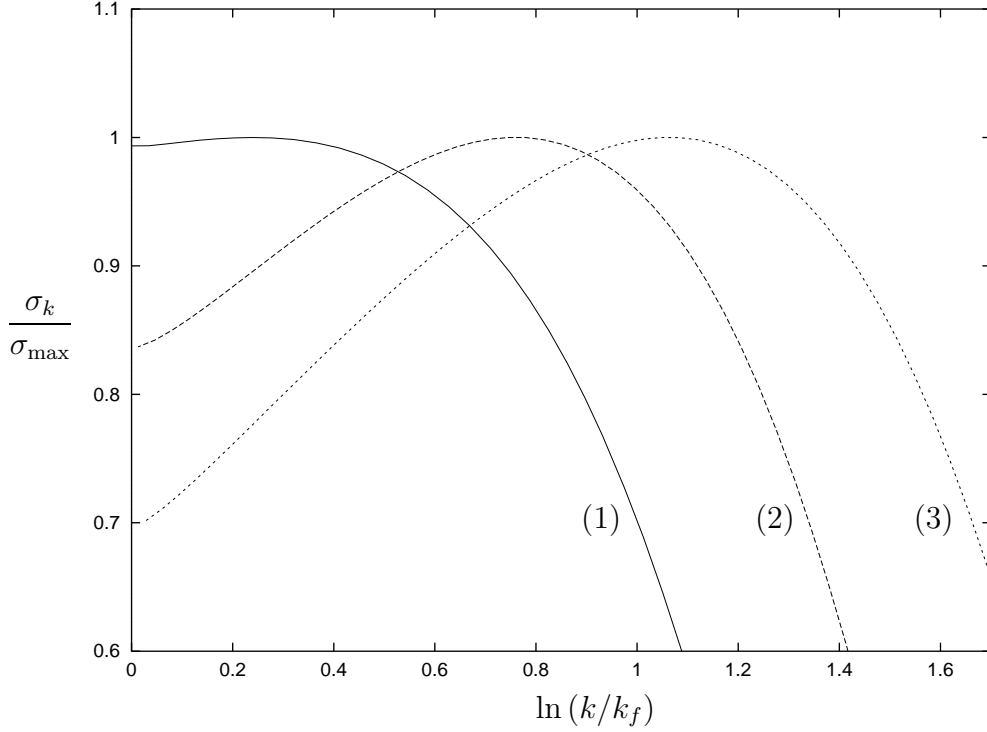


Figure 11: The normalized surface tension σ_k/σ_{\max} as a function of $\ln(k/k_f)$. The short distance parameters are (1) $\bar{\lambda}_{1\Lambda}/\Lambda = 0.1$, $\bar{\lambda}_{2\Lambda}/\Lambda = 2$, (2) $\bar{\lambda}_{1\Lambda}/\Lambda = 2$, $\bar{\lambda}_{2\Lambda}/\Lambda = 0.1$, (3) $\bar{\lambda}_{1\Lambda}/\Lambda = 4$, $\bar{\lambda}_{2\Lambda}/\Lambda = 70$.

this scale dependence is not taken into account correctly. If one takes the difference in σ_k from its maximum value to $\sigma_{k=k_f}$ as a rough measure for its uncertainty this is about 30% for the last example. Entering exponentially in eq. (9.4) this would lead to tremendous errors.

In order to quantify the differences between the three examples we have displayed some characteristic quantities in table 2. The renormalized couplings

$$\lambda_{1R} = U''_{k_f}(\rho_{0R}), \quad \lambda_{2R} = 4\partial_\tau U_{k_f}(\rho_{0R}) \quad (9.9)$$

are normalized to the mass term

$$m_R^c = (2\rho_{0R}\lambda_{1R})^{1/2}. \quad (9.10)$$

In addition we give the mass term

$$m_{2R}^c = (\rho_{0R}\lambda_{2R})^{1/2} \quad (9.11)$$

corresponding to the curvature of the potential in the direction of the second invariant τ . In comparison with figs. 9–11 one observes that the smaller the effective couplings the weaker the scale dependence of U_k and σ_k . In particular, a reasonably weak scale dependence of U_k and σ_k requires

$$\frac{\lambda_{1R}}{m_R^c} = \frac{1}{2} \frac{m_R^c}{\Delta\rho_{0R}} \ll 1. \quad (9.12)$$

$\frac{\bar{\lambda}_{1\Lambda}}{\Lambda}$	$\frac{\bar{\lambda}_{2\Lambda}}{\Lambda}$	$\frac{\lambda_{1R}}{m_R^c}$	$\frac{\lambda_{2R}}{m_R^c}$	$\frac{m_R^c}{m_{2R}^c}$	$\frac{m_R^c}{\Lambda}$	$\frac{m_{2R}^c}{\Lambda}$	$\frac{k_f}{\Lambda}$
0.1	2	0.228	8.26	0.235	1.55×10^{-1}	6.62×10^{-1}	1.011×10^{-1}
2	0.1	0.845	15.0	0.335	2.04×10^{-5}	6.10×10^{-5}	1.145×10^{-5}
4	70	0.980	16.8	0.341	6.96×10^{-2}	2.04×10^{-1}	3.781×10^{-2}

Table 2: The effective dimensionless couplings λ_{1R}/m_R^c and λ_{2R}/m_R^c . The couplings and the mass terms m_R^c , m_{2R}^c are evaluated at the scale k_f and $\delta\kappa_\Lambda = 0$.

This establishes a quantitative criterion for the range where Langer’s theory can be used without paying too much attention to the precise definition of the coarse graining. Comparison with fig. 5 (cf. sect. 4) shows that this condition is not realized for the range of couplings leading to universal behavior and for large $\bar{\lambda}_{1\Lambda}/\Lambda$. The only region where the saddle point expansion is expected to converge reasonably well is for small $\bar{\lambda}_{1\Lambda}/\Lambda$ and large $\bar{\lambda}_{2\Lambda}/\Lambda$. The second and the third example given in fig. 11, which exhibit a strong k -dependence, show similar values for the effective couplings. More precisely, for the relatively strong phase transition with slightly larger effective couplings one observes an increased scale dependence as compared to the weak phase transition. In table 2 also the renormalized masses in units of Λ which indicate the strength of the phase transition and k_f/Λ are presented.

In summary, we have shown that the coarse grained free energy cannot be defined without detailed information on the coarse graining scale k unless the effective dimensionless couplings are small. Only for small couplings we observe a weak k -dependence of the surface tension in a range where the location of the minima of the potential remains almost fixed. There is a close relation between the dependence of the coarse grained free energy on the coarse graining scale and the reliability of the saddle point approximation in Langer’s theory of bubble nucleation. For a strong k -dependence of U_k a small variation in the coarse graining scale can induce large changes in the predicted nucleation rate in lowest order in a saddle point approximation. In this case the k -dependence of the prefactor A_k has also to be computed. For strong dimensionless couplings a realistic estimate of the nucleation rate therefore needs the capability to compute $\ln A_k$ with the same accuracy as $16\pi\sigma_k^3/3\epsilon^2$ and a check of the cancelation of the k -dependence in the combined expression (9.4). Our observation that the details of the coarse graining prescription become less important in the case of small dimensionless couplings is consistent with the fact that typically small couplings are needed for a reliable saddle point approximation for A_k . For the electroweak high temperature phase transition a small k -dependence of σ_k is found for a small mass M_H of the Higgs scalar whereas for M_H near the W-boson mass the picture resembles our fig. 10 [42]. This corresponds to the observation [43, 44, 45] that the saddle point approximation around the critical bubble converges well only for a small enough mass of the Higgs scalar.

10 Conclusions

We have presented in this paper a detailed investigation of the phase transition in three dimensional models for complex 2×2 matrices. They are characterized by two quartic couplings $\bar{\lambda}_{1\Lambda}$ and $\bar{\lambda}_{2\Lambda}$. In the limit $\bar{\lambda}_{1\Lambda} \rightarrow \infty$, $\bar{\lambda}_{2\Lambda} \rightarrow \infty$ this also covers the model of unitary matrices. The picture arising from this study is unambiguous:

(1) One observes two symmetry breaking patterns for $\bar{\lambda}_{2\Lambda} > 0$ and $\bar{\lambda}_{2\Lambda} < 0$ respectively. The case $\bar{\lambda}_{2\Lambda} = 0$ denotes the boundary between the two phases with different symmetry breaking patterns. In this special case the theory exhibits an enhanced $O(8)$ symmetry. The phase transition is always first order for the investigated symmetry breaking $U(2) \times U(2) \rightarrow U(2)$ ($\bar{\lambda}_{2\Lambda} > 0$). For $\bar{\lambda}_{2\Lambda} = 0$ the $O(8)$ symmetric Heisenberg model is recovered and one finds a second order phase transition.

(2) The strength of the phase transition depends on the size of the classical quartic couplings $\bar{\lambda}_{1\Lambda}/\Lambda$ and $\bar{\lambda}_{2\Lambda}/\Lambda$. They describe the short distance or classical action at a momentum scale Λ . The strength of the transition can be parametrized by m_R^c/Λ with m_R^c a characteristic inverse correlation length at the critical temperature. For fixed $\bar{\lambda}_{2\Lambda}$ the strength of the transition decreases with increasing $\bar{\lambda}_{1\Lambda}$. This is analogous to the Coleman-Weinberg effect in four dimensions.

(3) For a wide range of classical couplings the critical behavior near the phase transition is universal. This means that it becomes largely independent of the details of the classical action once everything is expressed in terms of the relevant renormalized parameters. In particular, characteristic ratios like $m_R^c/\Delta\rho_{0R}$ (critical inverse correlation length in the ordered phase over discontinuity in the order parameter) or $m_{0R}^c/\Delta\rho_{0R}$ (same for the disordered phase) are not influenced by the addition of new terms in the classical action as far as the symmetries are respected.

(4) The range of short distance parameters $\bar{\lambda}_{1\Lambda}$, $\bar{\lambda}_{2\Lambda}$ for which the phase transition exhibits universal behavior is not only determined by the strength of the phase transition as measured by m_R^c/Λ . For a given $\bar{\lambda}_{1\Lambda}/\Lambda$ and small enough $\bar{\lambda}_{2\Lambda}/\Lambda$ one always observes universal behavior. In the range of small $\bar{\lambda}_{1\Lambda}/\Lambda$ the essential criterion for universal behavior is given by the size of $\bar{\lambda}_{2\Lambda}/\bar{\lambda}_{1\Lambda}$, with approximate universality for $\bar{\lambda}_{2\Lambda} < \bar{\lambda}_{1\Lambda}$. For strong couplings universality extends to larger $\bar{\lambda}_{2\Lambda}/\bar{\lambda}_{1\Lambda}$ and occurs for much larger m_R^c/Λ (cf. table 1).

(5) We have investigated how various characteristic quantities like the discontinuity in the order parameter $\Delta\rho_0$ or the corresponding renormalized quantity $\Delta\rho_{0R}$ or critical correlation lengths depend on the classical parameters. In particular, at the critical temperature one finds universal critical exponents for not too large $\bar{\lambda}_{2\Lambda}$,

$$\begin{aligned} \Delta\rho_{0R} &\sim (\bar{\lambda}_{2\Lambda})^\theta, & \theta &= 1.93, \\ \Delta\rho_0 &\sim (\bar{\lambda}_{2\Lambda})^{2\zeta}, & \zeta &= 0.988. \end{aligned} \tag{10.1}$$

These exponents are related by a scaling relation to the critical correlation length and order parameter exponents ν and β of the $O(8)$ symmetric Heisenberg model according to $\theta/\zeta = \nu/\beta = 1.95$ ($\nu = 0.882$, $\beta = 0.451$ in our calculation for $\bar{\lambda}_{2\Lambda} = 0$). Small values of $\bar{\lambda}_{2\Lambda}$ can be associated with a perturbation of the $O(8)$ symmetric model and θ, ζ

are related to the corresponding crossover exponents. On the other hand, $\Delta\rho_{0R}$ ($\Delta\rho_0$) becomes independent of $\bar{\lambda}_{2\Lambda}$ in the infinite coupling limit.

(6) We have computed the universal equation of state. The equation of state relates the derivative of the free energy U to an external source, $\partial U/\partial\varphi = j$. From there one can extract universal ratios e.g. for the jump in the order parameter ($\Delta\rho_{0R}/m_R^c = 0.592$) or for the ratios of critical correlation lengths in the disordered (symmetric) and ordered (spontaneously broken) phase ($m_{0R}^c/m_R^c = 0.746$). It specifies critical couplings ($\lambda_{1R}/m_R^c = 0.845$, $\lambda_{2R}/m_R^c = 15.0$). The universal behavior of the potential for large field arguments $\rho_R \gg \rho_{0R}$ is $U \sim \rho_R^3 \sim \rho^{3/(1+\eta)}$ provided ρ_R is sufficiently small as compared to Λ . Here the critical exponent η which characterizes the dependence of the potential on the unrenormalized field ρ is found to be $\eta = 0.022$. For large ρ the universal equation of state equals the one for the $O(8)$ symmetric Heisenberg model and η specifies the anomalous dimension or the critical exponent $\delta = (5 - \eta)/(1 + \eta)$. The equation of state is computed for a nonzero coarse graining scale k . It therefore contains information for quantities like the 'classical' bubble surface tension in the context of Langer's theory of bubble formation.

(7) We have investigated the dependence of the coarse grained effective potential $U_k(\rho)$ and the 'classical' surface tension σ_k on the coarse graining scale k with special emphasis on the question of the validity of Langer's theory of bubble formation. We find a strong scale dependence of U_k and σ_k if the phase transition is characterized by large dimensionless couplings. A weak scale dependence is observed for small effective couplings. There is a close relation between the dependence of the coarse grained free energy on the coarse graining scale and the reliability of the saddle point approximation in Langer's theory of bubble nucleation. A strong k -dependence of σ_k is only compatible with a large contribution from the higher orders of the expansion. We obtain a very consistent picture: The validity of the saddle point approximation typically requires small dimensionless couplings. In this case also the details of the coarse graining are not of crucial importance within an appropriate range of k . The quantitative criterion for the validity of Langer's formula is in our case $\lambda_{1R}/m_R^c \ll 1$.

(8) Our method is not restricted to the study of the universal behavior. We can compute the effective potential for arbitrary values of the initial parameters and have done this for particular examples.

The uncertainties of our results induced by the numerical integration of the flow equations are well under control and small. They are negligible compared to the expected error induced by our truncation. For a significant improvement of our treatment one would have to include higher order terms in the derivative expansion employed for the effective average action. For weak first order or second order phase transitions we expect the error to be related to the anomalous dimension $\eta = 0.022$. For the special case of the enhanced $O(8)$ symmetry one can compare e.g. with known values for critical exponents obtained by other methods [12, 46]. A comparison of our results for the critical exponents β and ν with the results of the most sophisticated calculations show agreement within a few per cent. The anomalous dimension is also well determined, even though it is most affected by our truncation.

Finally, we should mention that our approach can be extended in several directions. The generalization to complex $N \times N$ matrices for arbitrary N is straightforward. For large N this opens the possibility of a comparison with $1/N$ -expansions [47, 48]. Similarly, one may study systems with symmetry $U(N, N)$ or $U(2N)$ and symmetry breaking to the subgroup $U(N) \times U(N)$, relevant for the study of the metal insulator transition [1]. Very interesting generalizations are the systems with reduced $SU(N) \times SU(N)$ symmetry. They obtain by adding to the classical potential a term involving the invariant $\xi = \det \varphi + \det \varphi^\dagger$. (Note that ξ is not invariant with respect to $U(N) \times U(N)$). This will give an even richer pattern of phase transitions and permits a close contact to realistic meson models in QCD where the axial anomaly is incorporated. Finally one can extend the three dimensional treatment to a four dimensional study of field theories at nonvanishing temperature along the lines of ref. [6]. We hope to gain in this way new information about details of the chiral phase transition in QCD.

A Pole structure of the l_n^d integrals

The integrals

$$\begin{aligned} l_n^d(\omega) &= -n \int_0^\infty dy y^{\frac{d}{2}+1} \frac{\partial r(y)}{\partial y} [y(1+r(y)) + \omega]^{-(n+1)}, \\ \hat{l}_n^d(\omega) &= \frac{n}{2} \int_0^\infty dy y^{\frac{d}{2}} r(y) [y(1+r(y)) + \omega]^{-(n+1)} \end{aligned} \quad (\text{A.1})$$

with

$$r(y) = \frac{e^{-y}}{1 - e^{-y}} \quad , \quad \frac{\partial r(y)}{\partial y} = -\frac{e^{-y}}{(1 - e^{-y})^2} \quad (\text{A.2})$$

exhibit for $d \leq 2(n+1)$ a singularity at $\omega = -1$. The massless dimensionless average propagator $y(1+r(y))$ is a monotonic function of y that takes on its minimum at $y = 0$ with $\lim_{y \rightarrow 0} y(1+r(y)) = 1$. We define new variables δ and z ,

$$\delta = \omega + 1 \quad , \quad z = y(1+r(y)) - 1 \quad (\text{A.3})$$

and substitute in (A.1),

$$\begin{aligned} l_n^d(\delta) &= \int_0^\infty dz G_n^d(z) (z + \delta)^{-(n+1)}, \\ \hat{l}_n^d(\delta) &= \int_0^\infty dz \hat{G}_n^d(z) (z + \delta)^{-(n+1)} \end{aligned} \quad (\text{A.4})$$

with

$$\begin{aligned} G_n^d(z) &= -\frac{ny^{\frac{d}{2}+1} \frac{\partial r(y)}{\partial y}}{1 + r(y) + y \frac{\partial r(y)}{\partial y}}, \\ \hat{G}_n^d(z) &= \frac{ny^{\frac{d}{2}} r(y)}{2 \left(1 + r(y) + y \frac{\partial r(y)}{\partial y} \right)} \end{aligned} \quad (\text{A.5})$$

and $y = y(z)$. For $d < 2(n+1)$ the integrals (A.4) have a pole at $\delta = 0$. (The singularity becomes logarithmic in δ for $d = 2(n+1)$). In this case for $\delta \rightarrow 0$ the dominant contribution to the integral comes from the region $y \simeq 0$ or equivalently $z \simeq 0$. To find an approximate expression for l_n^d and \hat{l}_n^d near the pole we expand the regular part of G_n^d and \hat{G}_n^d around $z = 0$. With

$$\begin{aligned} r(y) &= \frac{1}{y} \left(1 - \frac{1}{2}y + \frac{1}{12}y^2 + O(y^4) \right), \\ \frac{\partial r(y)}{\partial y} &= -\frac{1}{y^2} \left(1 - \frac{1}{12}y^2 + O(y^4) \right) \end{aligned} \quad (\text{A.6})$$

one obtains

$$\begin{aligned} G_n^d(z) &= ny^{\frac{d}{2}-1} \left(2 - \frac{2}{3}y + \frac{1}{18}y^2 + O(y^3) \right), \\ \hat{G}_n^d(z) &= \frac{n}{2}y^{\frac{d}{2}-1} \left(2 - \frac{5}{3}y + \frac{13}{18}y^2 + O(y^3) \right). \end{aligned} \tag{A.7}$$

The inversion of $z(y)$ given by (A.3) can be done by expanding

$$z = \frac{1}{2}y + \frac{1}{12}y^2 + O(y^4) \tag{A.8}$$

and we find

$$y = 2z - \frac{2}{3}z^2 + \frac{4}{9}z^3 + O(z^4). \tag{A.9}$$

Insertion of (A.9) in (A.7) yields

$$\begin{aligned} G_n^d(z) &= 2n(2z)^{\frac{d}{2}-1} \left(1 - \frac{1}{3} \left(\frac{d}{2} + 1 \right) z + \left[\frac{1}{3} + \frac{1}{18} \left(\frac{d}{2} - 1 \right) \left(\frac{d}{2} + 6 \right) \right] z^2 + O(z^3) \right), \\ \hat{G}_n^d(z) &= n(2z)^{\frac{d}{2}-1} \left(1 - \frac{1}{3} \left(\frac{d}{2} + 4 \right) z + \left[2 + \frac{1}{18} \left(\frac{d}{2} - 1 \right) \left(\frac{d}{2} + 12 \right) \right] z^2 + O(z^3) \right). \end{aligned} \tag{A.10}$$

We consider for $d = 3$ and $n \geq 1$ the zeroth order expression for l_n^d and \hat{l}_n^d that obtains from the first term in (A.10) and the exchange of summation and integration in (A.4). Near the pole one finds

$$\begin{aligned} l_n^3(\delta) &\simeq 2^{3/2}n \int_0^\infty dz z^{1/2} (z + \delta)^{-(n+1)} \\ \hat{l}_n^3(\delta) &= \frac{1}{2}l_n^3(\delta). \end{aligned} \tag{A.11}$$

The leading contributions to l_1^3 , l_2^3 and l_3^3 are therefore given by

$$\begin{aligned} l_1^3(\delta) &= 2^{1/2}\pi\delta^{-1/2}, \\ l_2^3(\delta) &= 2^{-1/2}\pi\delta^{-3/2}, \\ l_3^3(\delta) &= 2^{-5/2}3\pi\delta^{-5/2}. \end{aligned} \tag{A.12}$$

We have verified this numerically.

References

- [1] F. Wegner, Z. Phys. **B35** (1979) 207; *ibid.* **38** (1980) 113; Phys. Rep. **67** (1980) 15; K.B. Efetov, A.I. Larkin and D.E. Kheml'nitskii, Soc. Phys. JETP **52** (1980) 568.
- [2] See e.g. P.G. de Gennes and J. Prost, *The physics of liquid crystals*, 2. ed. (Oxford, Clarendon Press, 1995).
- [3] For a recent review see P. Di Francesco, P. Ginsparg and J. Zinn-Justin, Phys. Rep. **254** (1995) 1.
- [4] D.-U. Jungnickel and C. Wetterich, hep-ph/9606483.
- [5] P. Ginsparg, Nucl. Phys. **B170** (1980) 388; T. Appelquist and R. Pisarski, Phys. Rev. **D23** (1981) 2305; S. Nadkarni, Phys. Rev. **D27** (1983) 917; N.P. Landsman, Nucl. Phys. **B322** (1989) 498.
- [6] N. Tetradis and C. Wetterich, Nucl. Phys. **B398** (1993) 659; Int. J. Mod. Phys. **A9** (1994) 4029.
- [7] K. Kajantie, M. Laine, K. Rummukainen, M.E. Shaposhnikov, Nucl. Phys. **B458** (1996) 90.
- [8] R.D. Pisarski and F. Wilczek, Phys. Rev. **D29** (1984) 338; F. Wilczek, Int. J. Mod. Phys. **A7** (1992) 3911; K. Rajagopal and F. Wilczek, Nucl. Phys. **B399** (1993) 395.
- [9] H. Meyer-Ortmanns, H.-J. Pirner and A. Patkos, Phys. Lett. **B295** (1992) 255; Int. J. Mod. Phys. **C3** (1992) 993; D. Metzger, H. Meyer-Ortmanns and H.-J. Pirner, Phys. Lett. **B321** (1994) 66; Phys. Lett. **B328** (1994) 547; H. Meyer-Ortmanns and B.-J. Schäfer, Phys. Rev. **D53** (1996) 6586.
- [10] R.D. Pisarski, hep-ph/9503330.
- [11] K.G. Wilson and M.E. Fisher, Phys. Rev. Lett. **28** (1972) 240.
- [12] J. Zinn-Justin, *Quantum Field Theory and Critical Phenomena* (Oxford University Press, 1993).
- [13] L.P. Kadanoff, Physica **2** (1966) 263.
- [14] K.G. Wilson, Phys. Rev. **B4** (1971) 3174; *ibid.* 3184; K.G. Wilson and I.G. Kogut, Phys. Rep. **12** (1974) 75; F.J. Wegner, in *Phase Transitions and Critical Phenomena*, vol. 6, eds. C. Domb and M.S. Greene, (Academic Press, 1976).
- [15] J. Berges, N. Tetradis and C. Wetterich, Phys. Rev. Lett. **77** (1996) 873.
- [16] M.M. Tsypin, Phys. Rev. Lett. **73** (1994) 2015; hep-lat/9601021.
- [17] J. Langer, Ann. Phys. **41** (1967) 108; *ibid.* **54** (1969) 258; Physica **73** (1974) 61.

- [18] C. Wetterich, Nucl. Phys. **B352** (1991) 529; Z. Phys. **C57** (1993) 451; *ibid.* **60** (1993) 461.
- [19] C. Wetterich, Phys. Lett. **B301** (1993) 90.
- [20] M. Bonini, M. D' Attanasio and G. Marchesini, Nucl. Phys. **B409** (1993) 441.
- [21] U. Ellwanger, Z. Phys. **C62** (1994) 503.
- [22] T. R. Morris, Phys. Lett. **B329** (1994) 241.
- [23] M. Reuter and C. Wetterich, Nucl. Phys. **B391** (1993) 147; *ibid.* **B408** (1993) 91; *ibid.* **417** (1994) 181; *ibid.* **427** (1994) 291; hep-th/9411227; M. Bonini, M. D' Attanasio and G. Marchesini, Nucl. Phys. **B418** (1994) 81; *ibid.* **421** (1994) 429; *ibid.* **437** (1995) 163; Phys. Lett. **B346** (1995) 87; U. Ellwanger, Phys. Lett. **B335** (1994) 364; U. Ellwanger, M. Hirsch and A. Weber, hep-ph/9606468.
- [24] F. Wegner and A. Houghton, Phys. Rev. **A8** (1973) 401; S. Weinberg in *Critical phenomena for field theorists*, Erice Subnucl. Phys. 1 (1976); J.F. Nicoll and T.S. Chang, Phys. Lett. **A62** (1977) 287; J. Polchinski, Nucl. Phys. **B231** (1984) 269; A. Hasenfratz and P. Hasenfratz, Nucl. Phys. **B270** (1986) 687.
- [25] F.J. Dyson, Phys. Rev. **75** (1949) 1736; J. Schwinger, Proc. Nat. Acad. Sci. **37** (1951) 452, 455.
- [26] A. Ringwald and C. Wetterich, Nucl. Phys. **B334** (1990) 506; N. Tetradis and C. Wetterich, Nucl. Phys. **B383** (1992) 197.
- [27] N. Tetradis and C. Wetterich, Nucl. Phys. **B422** [FS] (1994) 541.
- [28] D. U. Jungnickel and C. Wetterich, Phys. Rev. **D53** (1996) 5142.
- [29] S. Bornholdt, P. Büttner, N. Tetradis and C. Wetterich, cond-mat/9603129; S. Bornholdt, N. Tetradis and C. Wetterich, Phys. Rev. **D53** (1996) 4552.
- [30] M. Alford and J. March-Russell, Nucl. Phys. **B417** (1994) 527.
- [31] S. Coleman and E. Weinberg, Phys. Rev. **D7** (1973) 1888.
- [32] A. J. Paterson, Nucl. Phys. **B190** [FS3] (1981) 188; R. D. Pisarski and D. L. Stein, Phys. Rev. **B23** (1981) (3549); J. Phys. **A14** (1981) 3341; R. D. Pisarski and F. Wilczek, Phys. Rev. **D29** (1984) 338.
- [33] B. Bergerhoff, D. Litim, S. Lola and C. Wetterich, cond-mat/9502039; B. Bergerhoff, F. Freire, D. Litim, S. Lola and C. Wetterich, Phys. Rev. **B53** (1996) 5734.
- [34] P. Dreher, Phys. Lett. **B281** (1992) 127; Y. Shen, Nucl. Phys. **B** (Proc. Suppl.) **34** (1994) 712.

- [35] S. Y. Khlebnikov and R. G. Schnathorst, Phys. Lett. **B358** (1995) 81.
- [36] D.U. Jungnickel and C. Wetterich, hep-ph/9607411.
- [37] J. Adams, J. Berges, S. Bornholdt, F. Freire, N. Tetradis and C. Wetterich, Mod. Phys. Lett. A **10**, 2367 (1995).
- [38] B. Widom, J. Chem. Phys. **43** (1965) 3898.
- [39] J. Berges, C. Wetterich, in preparation.
- [40] S. Coleman, Phys. Rev. **D15** (1977) 2929; C. Callan and S. Coleman, Phys. Rev. **D16** (1977) 1762.
- [41] A.D. Linde, Nucl. Phys. **B216** (1983) 421.
- [42] N. Tetradis, hep-ph/9608272.
- [43] J. Kripfganz, A. Laser and M.G. Schmidt, Nucl. Phys. **B433** (1995) 467; hep-ph/9512340.
- [44] W. Buchmüller, Z. Fodor, T. Helbig and D. Walliser, Ann. Phys. **234** (1994) 260; D. Bödeker, W. Buchmüller, Z. Fodor and T. Helbig, Nucl. Phys. **B423** (1994) 171.
- [45] J. Baacke, Phys. Rev. **D52** (1995) 6760.
- [46] P. Butera and M. Comi, hep-lat/9505027; T. Reisz, hep-lat/9507011.
- [47] G. Ferretti, Nucl. Phys. **B450** [FS] (1995) 713.
- [48] S. Nishigaki, Phys. Lett. **B376** (1996) 73.